Journal of Medicinal Chemistry

Article

pubs.acs.org/jmc

Efficacious Inhaled PDE4 Inhibitors with Low Emetic Potential and Long Duration of Action for the Treatment of COPD

Chris De Savi,*[,†,‡] Rhona J. Cox,*[,†,§] Daniel J. Warner,[†] Anthony R. Cook,[†] Mark R. Dickinson,[†] Amy McDonough,[†,∥] Louis C. Morrill,[†] Beth Parker,[†] Glen Andrews,[†] Simon S. Young,[†,∥] Peter S. Gilmour,[†,∥] Rob Riley,[†,∥] and Matthew S. Dearman[†,§]

[†]AstraZeneca R&D Charnwood, Loughborough, Leicestershire, LE11 5RH, U.K.

[‡]Oncology iMed, AstraZeneca R&D Boston, 35 Gatehouse Drive, Waltham, Massachusetts 02451, United States

[§]Respiratory, Inflammation & Autoimmunity iMed, AstraZeneca R&D Mölndal, Pepparedsleden, 431 83 Mölndal, Sweden

[∥]AstraZeneca, Mereside, Alderley Park, Macclesfield, Cheshire, SK10 4TG, U.K.

Supporting Information

ABSTRACT: Oral phosphodiesterase 4 (PDE4) inhibitors, such as cilomilast and roflumilast, have been shown to be efficacious against chronic obstructive pulmonary disease (COPD). However, these drugs have been hampered by mechanism-related side effects such as nausea and emesis at high doses. Compounds administered by inhalation are delivered directly to the site of action and may improve the therapeutic index required to overcome side effects. This paper describes systematic and rational lead optimization to deliver highly potent, long-acting, and efficacious preclinical inhaled PDE4 inhibitors with low emetic potential.

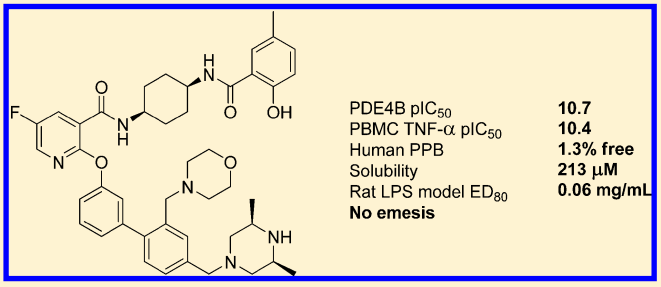

INTRODUCTION

Chronic obstructive pulmonary disease (COPD) is characterized by persistent airflow limitation that is usually progressive and is associated with an enhanced chronic inflammatory response in the airways and lungs to noxious particles and gases.[1] It is a major public health burden, with a global prevalence of 10.1%,[2] causing 3 million deaths worldwide in 2011[3] and predicted to be the fourth leading cause of death by 2030.[4] The economic burden associated with the disease is substantial, with the total costs of COPD in the U.S. estimated at $49.8 billion in 2010.[5] COPD-associated inflammation responds only weakly to corticosteroids,[6] and new treatments are urgently required.

Phosphodiesterase 4 (PDE4) hydrolyzes the phosphodiester bond of cAMP to produce inactive AMP. Inhibitors of PDE4 elevate intracellular cAMP concentration, which leads to activation of specific protein phosphorylation cascades. These in turn reduce a wide variety of inflammatory mediators and inflammatory cell functions.[7] PDE4 inhibitors reduce pulmonary inflammation and improve lung function in preclinical models of asthma and COPD, and several PDE4 inhibitors have advanced into clinical trials for the treatment of COPD and other inflammatory diseases.[8]

Most clinical investigations have focused on oral delivery of PDE4 inhibitors. The first-generation inhibitor *R*-rolipram (**1**) caused emesis, a mechanistic side-effect of PDE4 inhibitors, at effective anti-inflammatory doses.[9] More recently, second-generation inhibitors cilomilast (**2**)[10] and roflumilast (**3**)[11] have shown clinical efficacy, and roflumilast has a superior therapeutic index over emesis. However, nausea and vomiting still limit the oral dose of PDE4 inhibitors (Figure 1).

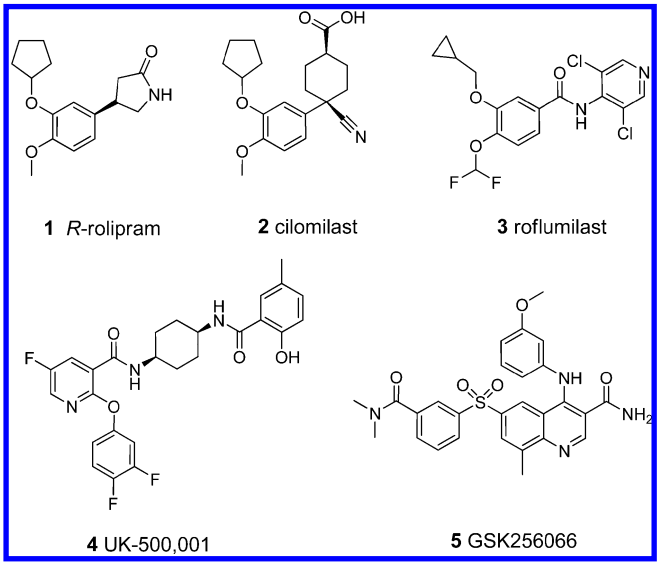

Figure 1. Representative oral and inhaled PDE4 inhibitors.

Received: January 23, 2014

dx.doi.org/10.1021/jm5001216 | J. Med. Chem. XXXX, XXX, XXX−XXX

Drugs to treat respiratory diseases can be inhaled, which reduces systemic exposure and associated side effects. Pfizer and GlaxoSmithKline have both reported inhaled PDE4 inhibitors which have progressed to the clinic. Others have also recently reported the design and discovery of novel inhaled PDE4 inhibitors.[12,13] Pfizer's UK-500,001 (**4**) showed preclinical efficacy in a variety of species but has since been discontinued because of lack of efficacy in patients suffering from moderate to severe COPD.[14] Although the drug was generally well tolerated, mechanism-related side effects were observed in the higher dose groups. GSK256066 (**5**) was in clinical development for allergic rhinitis, asthma, and COPD but is not currently listed in the company's pipeline. It is very potent in vitro and has demonstrated potent and long-lasting anti-inflammatory effects in animal models of pulmonary inflammation.[15] Furthermore, no emesis has been reported in a ferret model.[16] Clinically, **5** significantly reduced early and late stage asthmatic response to allergen challenge in mild asthmatics after 1 week of treatment.[17]

RESULTS AND DISCUSSION

In Vitro and in Vivo Data for 4 and 5. The medicinal chemistry strategy adopted by GSK was to deliver an exquisitely potent PDE4 compound with low aqueous solubility and oral bioavailability.[18] The Pfizer strategy appeared to focus on both high metabolic clearance and high plasma protein binding to minimize systemic exposure (Table 1).

Table 1. AstraZeneca Data Generated on 4 and 5

property	4	5
human PDE4B enzyme pIC_{50}[a]	9.2 (6)	>11 (2)
PBMC TNF-α pIC_{50}[a]	8.4 (10)	11.5 (7)
human whole blood TNF-α pIC_{50}[a]	NT	9.5 (9)
rat whole blood TNF-α pIC_{50}[a]	7.4 (2)	9.6 (2)
PPB %free human/rat[a]	0.17/1.7 (1)	1.5/2.4 (1)
aqueous solubility pH 7.4 (μM)[a]	<1 (1)	1.2 (1)
MW/clogP/log D[a]	500/5.3/4.4 (1)	519/3.8/2.7 (1)
human microsomal Cl_{int} (μL/min/mg)[a]	116 (1)	>150 (1)
rat hepatocyte Cl_{int} (μL/min/10^6 cells)[a]	76 (1)	130 (1)
rat pharmacokinetics at 1 mg/kg:[b]		
Cl (mL/min/kg)	97	32
V_{dss}/V_z (L/kg)	22/63	0.75/40
iv $t_{1/2}$ (h)	7.6	14.9
i.t. $t_{1/2}$ (h)	NT	8.1
in vivo efficacy in rat (inhaled):[c]		
LPS DRC; lowest efficacious nebulizer concentration (LENC)	inactive at all doses	0.03 mg/mL
LPS duration	NT	inactive

[a]Numbers of replicates are stated in brackets. [b]n = 2−3 animals. [c]Data from a single experiment, n = 8−10 animals per treatment group. NT = not tested.

In our assays, **4** was rapidly metabolized and had high plasma protein binding and was therefore likely to achieve very low systemic exposure. It was inactive in our rat pulmonary inflammation model when administered as a nebulized aerosol (Figure S1A, Supporting Information). An increase in the lung-delivered dose of **4** when administered by dry powder aerosol resulted in, at best, inconsistent inhibition of LPS-induced neutrophilia (Figure S1B, Supporting Information) despite significant deposited lung doses (Figure S1C, Supporting Information). We have hypothesized that the lack of activity seen for **4** in our in-house rat lung inflammation models could be due to its moderate potency. High total lung concentrations were not able to compensate for this potency in these experiments, potentially as a consequence of low solubility.

In our model, **5** had a variable effect on lung neutrophilia with no clear dose response. It inhibited lung neutrophilia at 0.03 mg/mL equivalent nebulizer concentration, resulting in a measured terminal lung concentration of 38 nM. No significant effects were observed at 0.01 or 0.1 mg/mL (Figure S2A, Supporting Information). No doses of **5** resulted in significant inhibition of lung inflammation when dosed 12 h before the inflammatory challenge despite the highest dose achieving total lung concentrations of up to 356 nM (Figure S2B, Supporting Information). The reason for the variable efficacy of **5** is not clear; the lack of a relationship between compound level and biological effect is surprising. We have hypothesized that the lack of significant activity of **5** at 12 h could be due to an inconsistent availability of free compound in the biophase and activity associated with poorly soluble compound in the lung,[19] similar to **4**. However, we cannot discount that using a different formulation or in vivo model may lead to different results. Studies by GSK on LPS-induced lung inflammation in rats showed that high levels of **5** were seen in lung tissue up to 40 h, when the inflammatory effect had declined.[16] GSK has suggested that **5** is retained in lung tissue because of the lipophilic nature of this compound, but there is little relationship between lung matrix levels of **5** and duration of anti-inflammatory effect. It is likely that high levels of **5** are being retained in the lung but that the majority of compound is either in solid form and/or in lipid compartments in the lung and the levels of free compound in the intracellular cytoplasm (the site of PDE4) are too low to exert a pharmacological effect.

Design. Our strategy was also to reduce mechanism-based side effects by limiting systemic exposure, but the overall preclinical profile of our compounds differed. We aimed to find compounds with high whole blood potency to give a low (<15 μg/kg) predicted dose to man, along with high solubility (>50 μM) and >8 h half-life in rat in vivo iv PK, which correlates well with *i.t.* PK.[20] Low free fraction in human plasma (<5%) and low preclinical bioavailability should limit systemic exposure and reduce emetic potential. While there are some reports suggesting that inhibition of subtype PDE4B leads to anti-inflammatory effects and that inhibition of PDE4D causes emesis,[21] we felt that it would be difficult to achieve sufficiently high margins using this approach. Additionally, we required appropriate solid state properties for inhalation, i.e., high crystallinity, low hygroscopicity, no low temperature thermal events, and micronizable for use in a dry powder inhaler. Together with in vivo activity in both LPS dose response and duration experiments, we believed this profile would provide confidence in a once daily predicted inhaled dose in the clinic.

We have previously disclosed several series of both neutral and basic highly potent pyridopyrimidinedione PDE4 inhibitors for inhaled delivery,[22,23] of which **6** and **7** are representative examples (Figure 2). This paper describes the search for a structurally differentiated back-up series.[24]

During the early phases of the project, a significant number of pyridopyrimidinediones were profiled in our LPS dose response assays. At the time, there was no method to confidently predict whether a compound would show efficacy and subsequent duration of effect, so a statistical analysis was undertaken to identify potential measurable parameters that could be used to prioritize compounds for in vivo studies.

dx.doi.org/10.1021/jm5001216 | J. Med. Chem. XXXX, XXX, XXX−XXX

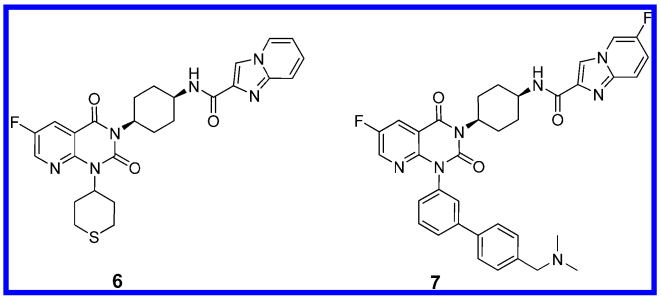

Figure 2. Representative examples of earlier AstraZeneca PDE4 inhibitors.

Initial quantitative analysis of in vivo efficacy used internal compounds from the earlier lead optimization program,[23] supplemented by a diverse set of published PDE4 inhibitors, comprising 41 compounds in total. Compounds were qualitatively flagged as active or inactive, according to whether they had exhibited significant efficacy at any of the concentrations screened in single or multiple dose studies. Nominal logistic regression was used to independently fit nine in vitro physicochemical and PK parameters and three in vivo PK parameters to the qualitative activity flags using JMP.[25] The two parameters exhibiting the most significant correlation (pIC_{50} in PBMC and $t_{1/2}$ from rat iv studies, $p < 0.001$ in both cases) were then used in combination to estimate the probability of observing activity in vivo:

$$P(\text{activity in DRC}) = \frac{1}{1 + e^{15.85-(1.47\times pIC_{50})-(3.83\times \log_{10}(t_{1/2}))}} \quad (1)$$

Substituting the PBMC pIC_{50} and $t_{1/2}$ of **5** into the above equation gives a >99% chance of activity, whereas the equivalent substitutions for **4** suggest a 47% chance. A graphical representation of this model is provided (Figure S3(a), Supporting Information).

For the purposes of quantitative analysis, the in vivo efficacy of the compounds was represented by the lowest effective nebulizer concentration (LENC), i.e., the lowest nebulizer concentration at which significant efficacy was observed, expressed as:

$$\text{pLENC} = -\log_{10}(\text{LENC}) \quad (2)$$

Using linear regression, we screened the same 12 parameters as above for statistically significant relationships with pLENC for the subset of 26 active compounds. In contrast to the qualitative analysis, quantitative analysis revealed just two statistically significant relationships: the pIC_{50} values from the enzyme and cell potency (PBMC) assays ($p = 0.005$ and $p = 0.011$, respectively). As the correlation between these two parameters themselves is very high, we opted to base our predictions on the cellular assay alone, allowing us to estimate the LENC according to the following equation (Figure S3(b), Supporting Information):

$$\text{predicted pLENC} = 0.48 \times pIC_{50}(\text{PBMC}) - 1.16 \quad (3)$$

This relationship was heavily based on 24 internal compounds, as just two reference compounds (**2** and **5**) exhibited quantifiable activity in our in vivo model. Thus, from the initial analysis, we were able to identify cell potency and half-life as qualitative markers of efficacious compounds. Within those predicted to be active, we could then quantitatively estimate the LENC based on the cellular potency alone. Dose ranges used in dose response experiments were determined from these estimated LENC values.

The nominal logistic regression approach was also applied to 20 compounds previously prioritized for duration experiments to determine whether any of the same parameters were capable of discriminating actives from inactives at the later time point. On the basis of this analysis (and given that each compound had previously shown activity in terms of a dose response), we were able to estimate the probability of a compound exhibiting duration of action as a function of log D (Figure S3(c), Supporting Information):

$$P(\text{duration of activity}) = \frac{1}{1 + e^{(1.77\times \log D)-4.45}} \quad (4)$$

The probability of retaining efficacy for a 12 h period drops sharply as the log D increases from 2 (71%) to 3 (29%). This allowed us, on the basis of a single in vitro parameter, to prioritize only those compounds with the greatest chance of demonstrating 12 h duration, and focus efforts on compounds with equivalent or lower log D than **5** (log D = 2.7, 54% chance of achieving duration).

It was known from earlier work independently conducted by AstraZeneca and by Pfizer that a bicyclic or pseudobicyclic fluoropyridine core substituted by a lipophilic aromatic ring and a *cis*-1,4-diaminocyclohexane are beneficial for potency.[22,23,26] During development of our biaryl series (**7**), we discovered that addition of a base to the biaryl can significantly enhance solubility. Furthermore, detailed profiling of different chemical classes across a range of inhaled programs has demonstrated that bases, and dibases in particular, can provide a long duration in the rat lung following *i.t.* administration.[27] Compound **8a** (Figure 3, Table 2)

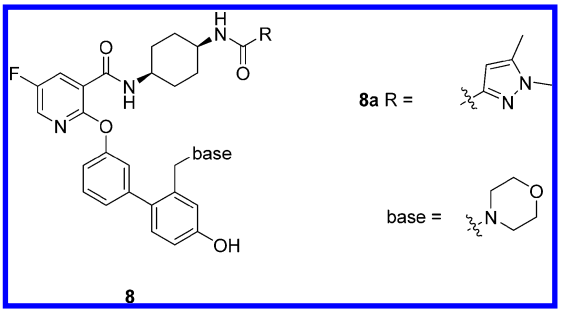

Figure 3. Structure of lead compound **8a**.

Table 2. Properties of Lead Compound 8a

property	8a
human PDE4B pIC_{50}	10.8
PBMC TNF-α pIC_{50}	10.2
human PPB % free	5.6
aqueous solubility pH 7.4 (μM)	250
log D	3.1
CYP pIC_{50} (4 isoforms)	<6.0 except 3A4 6.3, 2C9 6.6
rat iv PK $Cl/V_{dss}/V_z/t_{1/2}$ (h)	69/2.6/76/13
in vivo LPS DRC; LENC	active at 0.1 mg/mL
in vivo LPS duration; LENC	active at 0.1 mg/mL

was discovered during our first lead optimization phase and appeared to be a good start point for a back-up program.

Variation of the amide and replacements for the morpholine to decrease the plasma free fraction were investigated first (**8**).

dx.doi.org/10.1021/jm5001216 | J. Med. Chem. XXXX, XXX, XXX−XXX

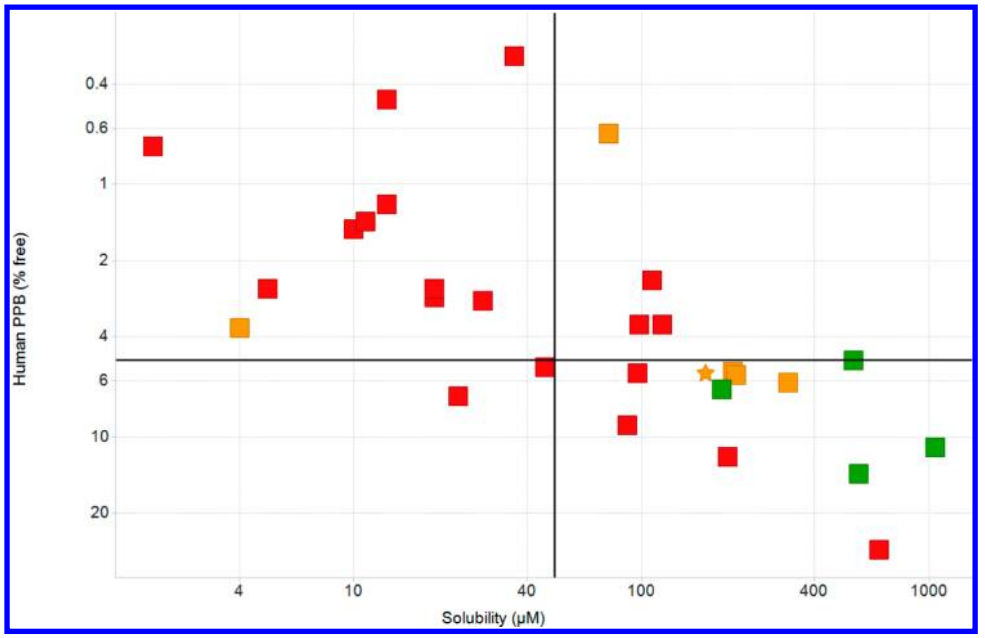

Figure 4. Variation of solubility and PPB by changing both the amide and base in structure **8**. Colors illustrate CYP3A4 activity (pIC_{50} > 6.5, red; 6.0 < pIC_{50} < 6.5, orange; pIC_{50} < 6.0, green). All compounds have PDE4B pIC_{50} > 9.5. Star shows **8a**.

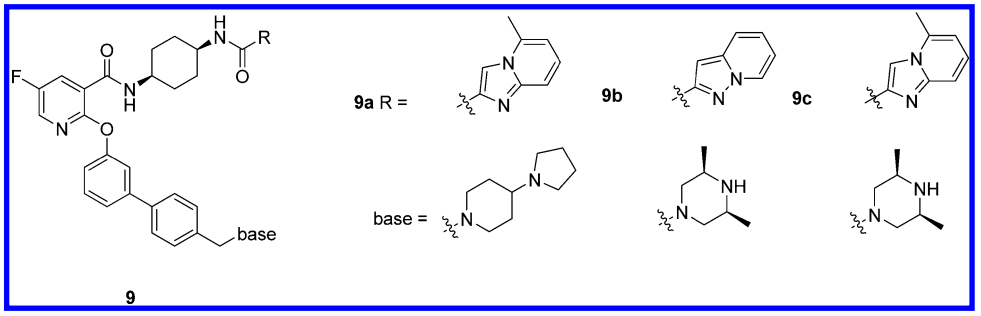

Figure 5. Structures of *para*-benzylamines.

In raising lipophilicity, CYP inhibition increased and solubility decreased to unacceptable levels. A correlation between solubility and plasma-free fraction suggested that there would be difficulty in achieving both solubility >50 μM and free fraction <5% in this subseries (Figure 4). A key finding was that potency was only retained if the *ortho*-position was substituted with weak bases of limited size. However, compound **8a** and analogues with a weak base in the *ortho*-position generally did not show good efficacy in the LPS DRC model despite a 96% predicted likelihood of activity. Morpholine **8a** did show efficacy (37% reduction in LPS-induced bronchoalveolar lavaged neutrophils) at 0.1 mg/mL but at higher concentrations the inhibition was lost, suggesting a possibility of local irritancy masking the efficacy readout at higher doses.

In parallel, we explored compounds with a *para*-benzylamine on the biaryl and no *ortho*-substituent (**9**) (Figure 5). In this case, CYP inhibition was a less significant problem and we were able to raise the log *D* to achieve a low free fraction. Potency in the PBMC assay was generally lower than with an *ortho*-benzylamine, with the highest potencies in this subseries being achieved with *para*-piperazines. Addition of two methyl groups to the piperazine reduced the PPB free fraction without detrimentally affecting other properties (Figure 5, Table 3).

Potency SAR for the amide appears to be broadly parallel between the *ortho*- and *para*-benzylamine series, as illustrated by the matched pairs in Table 4. The presence of an acceptor (−N=) either adjacent to the amide carbonyl or in a fused ring was important for high potency, although 2-phenolic compounds are also potent. The effects of the phenol and nitrogen acceptor are not additive, suggesting that the two features are involved in the same binding site interaction.

Substitution of the biaryl with a benzylamine in the *meta*-position generally led to a drop in potency compared to the

Table 3. Properties of Key Compounds from *para*-Benzylamine Subseries

property	9a	9b	9c
human PDE4B pIC_{50}	10.4	10.6	10.2
PBMC TNF-α pIC_{50}	9.6	10.1	9.9
human PPB (% free)	2.0	4.5	1.2
aqueous solubility pH 7.4 (μM)	>1400	580	460
log *D*	3.2	2.7	2.7
CYP pIC_{50} (5 isoforms)	all <6.0	<6.0 except 3A4 6.4	all <6.0
rat iv PK Cl/V_{dss}/V_z/$t_{1/2}$ (h)	79/60/80/12	58/13/30/5.8	61/14/28/5.3
in vivo LPS DRC; LENC	active at 1 mg/mL	active at 0.03 mg/mL	NT

dx.doi.org/10.1021/jm5001216 | J. Med. Chem. XXXX, XXX, XXX−XXX

Table 4. PDE4B Enzyme pIC_{50}: Representative Examples to Illustrate SAR

	ortho-benzylamine **8** (Figure 3)			*para*-benzylamine **9** (Figure 5)		
base R	morpholine	dimethyl-amine	homo-morpholine	*cis*-2,6-dimethyl-piperazine	dimethyl-amine	homo-morpholine
	10.8 (**8a**)		11.0 (**8b**)	10.6 (**9d/10a**)		
	10.6 (**8c**)	10.5 (**8d**)	10.7 (**8e**)	10.2 (**9e**)	9.4 (**9f**)	10.0 (**9g**)
	10.8 (**8f**)			10.5 (**9h**)		
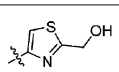	10.2 (**8g**)			10.1 (**9i**)		
		10.5 (**8h**)	10.7 (**8i**)			
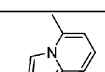	10.8 (**8j**)	10.3 (**8k**)	10.5 (**8l**)	10.2 (**9c**)	9.1 (**9j**)	9.9 (**9k**)
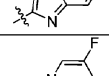		10.3 (**8m**)	10.7 (**8n**)	10.0 (**9l**)		
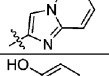	10.6 (**8o**)		10.5 (**8p**)			
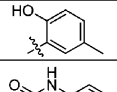	9.5 (**8q**)					
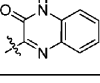	9.9 (**8r**)			9.9 (**9m**)		
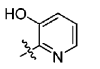	8.6 (**8s**)					
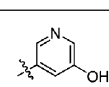	10.3 (**8t**)					
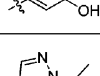		10.3 (**8u**)				
		9.5 (**8v**)				
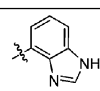		7.7 (**8w**)				

corresponding *para*-benzylamines. As no other obvious advantages were noted, this subseries was not explored further.

Combination of *meta*- or *para*-benzylamines with a phenolic hydroxyl was also investigated to see if this group could be used to reduce plasma free fraction (Figure 6, Table 5). In the case of the *meta*-benzylamines, addition of a *para*-hydroxyl led to an increase in potency but no dramatic change in plasma binding. Installation of the hydroxyl in other sites around the aryl ring showed significant drops in cell potency. Addition of a *meta*-hydroxyl to a *para*-benzylamine was generally tolerated, but again there was no plasma binding advantage. In addition, many of the hydroxylated benzylamines also carried the theoretical possibility of elimination of the basic group to form a quinone methide, which was viewed as an undesirable liability.

Our statistical analysis showed that critical properties needed for both efficacy and duration were high PBMC pIC_{50} (ideally >9.5), low log *D*, and long half-life (ideally >8 h) in rat PK. While we had achieved the first two, many compounds synthesized thus

dx.doi.org/10.1021/jm5001216 | *J. Med. Chem.* XXXX, XXX, XXX−XXX

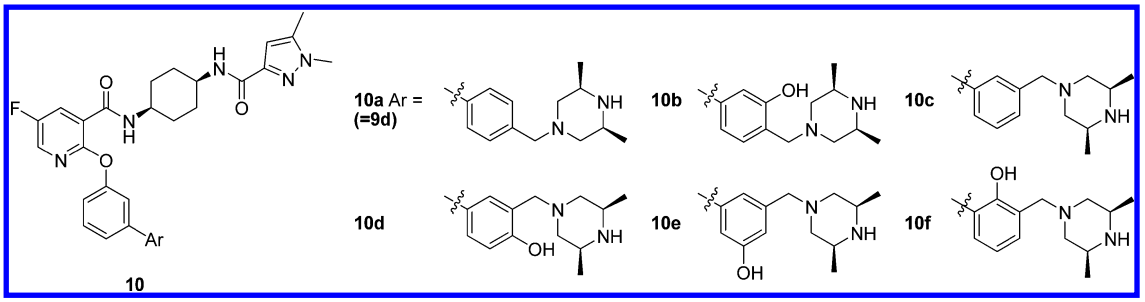

Figure 6. Substitution on the biaryl with hydroxyl groups.

Table 5. Effects of Hydroxylating the Biaryl

property	10a (= 9d)	10b	10c	10d	10e	10f
human PDE4B pIC_{50}	10.6	10.5	10.2	10.7	10.5	10.1
PBMC TNF-α pIC_{50}	10.0	10.5	10.1	10.4	9.4	8.5
human PPB (% free)	11	12	18	16	35	9.1
aqueous solubility pH 7.4 (μM)	1300	890	>1500	970	>1500	470
log *D*	2.4	2.4	2.1	2.3	2.2	2.8

far in the project had shown insufficiently long half-life for progression into efficacy models. In vivo clearance of these compounds was generally at the rate of liver blood flow, so an increased volume of distribution (V_z) was needed to prolong half-life. Because the enzyme binding site appeared to be tolerant of a wide variety of base positions, the chain length in both *para* and *meta* positions was extended to position the base further from the biaryl unit and increase basicity. We predicted this would increase V_z. Low PBMC potency was an issue for many examples, but a number of those compounds with PBMC pIC_{50} > 10 progressed to rat iv PK, showing increased V_z and correspondingly longer half-lives (Figures 7 and 8).

We were also pleased to discover that these extended bases showed higher plasma binding for equivalent log *D* when compared to earlier compounds, which meant they were more likely to show both <5% free in plasma and 12 h duration (Figure 9).

Potency, plasma binding, rat iv PK half-life, and measured log *D* were used to prioritize compounds for efficacy and duration studies. Two lead compounds (**11a** and **11e**) (Table 6) were investigated further and showed suitable margins in in vitro toxicology assays. The crystallinity of **11a** was investigated and the free base was found to be crystalline though hygroscopic.

Dibasic compounds made earlier in the project had been shown to have a 12 h duration of action despite having higher log *D* than the top limit for duration in the monobase series. We proposed a further subseries of compounds with bases in both the *ortho*- and *para*-positions (**12**) and speculated that these compounds should have high potency, low plasma free fraction, robust PK and efficacy properties, and perhaps also the potential for good solid-state properties (Figure 10). For example, earlier work suggested that compounds with an *ortho*-benzylamine tended to crystallize easily to give a nonhygroscopic polymorph.

The results of the first set of *ortho*,*para*-dibases to be synthesized showed good activity in both enzyme and cell assays but lacked sufficiently high plasma protein binding to meet our criteria for a clinical candidate. We capitalized on the extensive knowledge that had already been established in terms of enzyme activity and human PPB in order to increase PPB in the dibasic series. Of 1680 compounds with measured PDE4 enzyme potency, 581 matched the fragmentation scheme depicted in Figure 11 (top left) and could therefore be used in the model construction. From this scheme we were able to identify three unique "cores", 171 "top", and 185 "bottom" fragments. A Free–Wilson model[28] for potency was built with a training set R^2 of 0.93 and RMSE of 0.22, which we were then able to use to predict the activity of $(3 \times 171 \times 185) = 94905$ virtual structures. As we were particularly interested in increasing the plasma binding of a specific subseries (Figure 11, center right), we quickly narrowed this library to just 171 potential compounds for synthesis, featuring each of the "top" fragments identified above. This virtual library covered a range of predicted activities from the Free–Wilson model and was filtered on predicted $pIC_{50} \geq 10.2$. Plasma protein binding was predicted[29] for the 20 virtual structures that remained upon filtration, and the results were visualized as shown to the bottom left of Figure 11. Compounds that had been synthesized prior to that point (in red) occupy the bottom left of the plot, i.e., they have comparatively low potency and plasma binding. Conversely, there are a number of points situated to the top right of the plot which offered potential avenues for increasing either of these two parameters or even

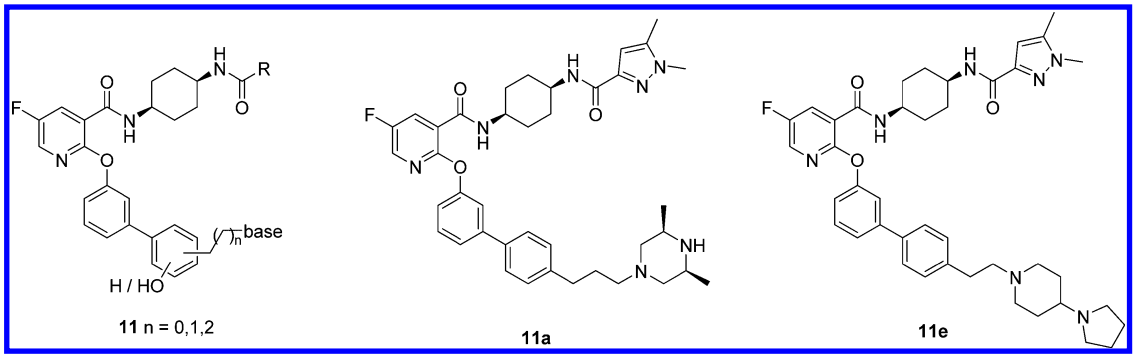

Figure 7. Structures of extended bases.

dx.doi.org/10.1021/jm5001216 | J. Med. Chem. XXXX, XXX, XXX–XXX

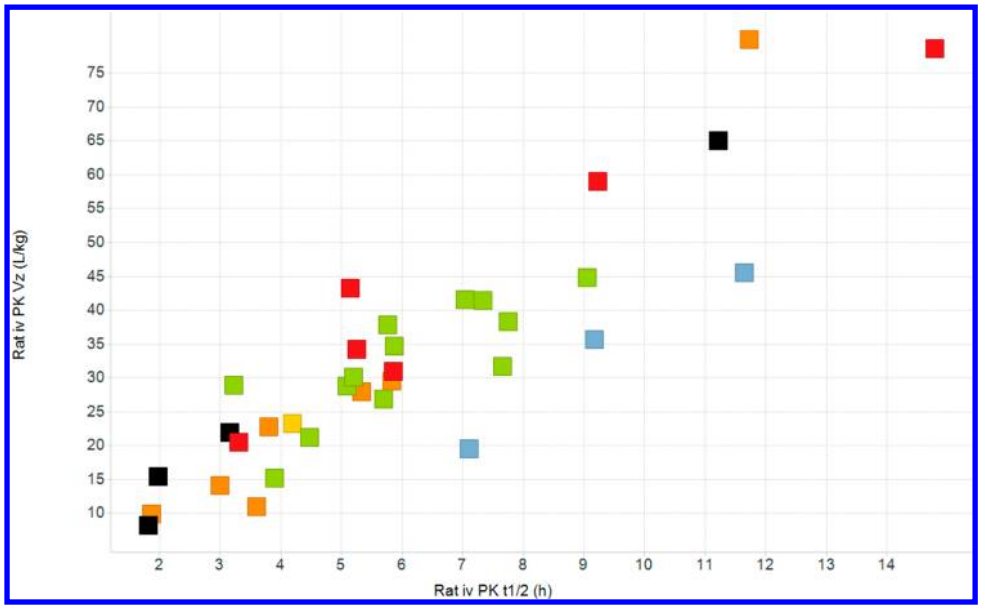

Figure 8. Relationship between rat iv PK half-life and V_z, colored by compound class (**11**). Orange = *para*, $n = 0$; yellow = *meta*, $n = 0$; black = *ortho*, $n = 0$; red = *para*, $n = 1$; purple = *meta*, $n = 1$; green = *para*, $n = 2$; blue = *meta*, $n = 2$.

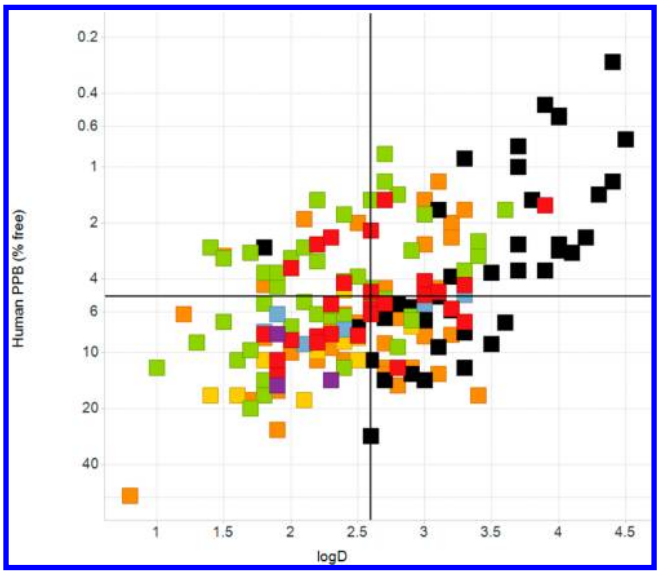

Figure 9. Variation of plasma binding with log *D* colored by compound class as in Figure 8.

both. The compounds shown in blue were selected for synthesis (Figure 11, bottom right) and this final set of *ortho*,*para*-dibasic compounds was prepared.

Chemistry. All compounds described in this paper were synthesized from a common intermediate **13** which was made by amide coupling of chloronicotinic acid **14** to Boc-protected amine **15**[26] using propylphosphonic anhydride (T3P) followed by displacement of chloride by 3-iodophenol (Scheme 1).

The first compound in the series, **8a**, was prepared by deprotection of **13** and amidation, followed by Suzuki coupling of aryl boronic acid **16** (Scheme 2).

For later compounds, we developed a flexible and high yielding synthetic strategy which allowed parallel investigation of either end of the molecule; **13** could either be deprotected and amidated, followed by Suzuki coupling then functionalization with a variety of amines (route I) or Suzuki coupling and amine

Table 6. Properties of Advanced Compounds with Extended Bases

property	11a	11e
human PDE4B pIC_{50}	10.7	10.4
PBMC TNF-α pIC_{50}	10.2	10.5
human PPB (% free)	4.5	4.2
aqueous solubility pH 7.4 (μM)	130	120
log *D*	2.6	2.4
rat iv PK Cl/V_{dss}/V_z/$t_{1/2}$ (h)	68/21/41/7	74/44/59/9
CYP pIC_{50} (5 isoforms)	all <6.0	all <6.0
in vivo LPS DRC; LENC	0.03 mg/mL	0.1 mg/mL
ED_{80} (nebulizer concentration/lung concentration/lung deposited dose)	0.05 mg/mL/60 nM/0.6 μg/kg	ND
in vivo LPS duration; LENC	active at 0.1 mg/mL	active at 0.1 mg/mL

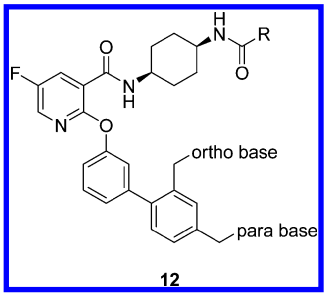

Figure 10. Structure of *ortho*,*para*-dibases.

formation carried out first, followed by amidation with a variety of acids (route II).

Routes I and II were generally comparable in terms of ease and overall yield, as illustrated by the synthesis of *para*-benzylamines for which both routes were used (Scheme 3).

Sometimes it was more efficient to convert the aryl iodide to the corresponding boronic ester if the second aryl unit was more readily available as the halide, which was often the case for

dx.doi.org/10.1021/jm5001216 | J. Med. Chem. XXXX, XXX, XXX−XXX

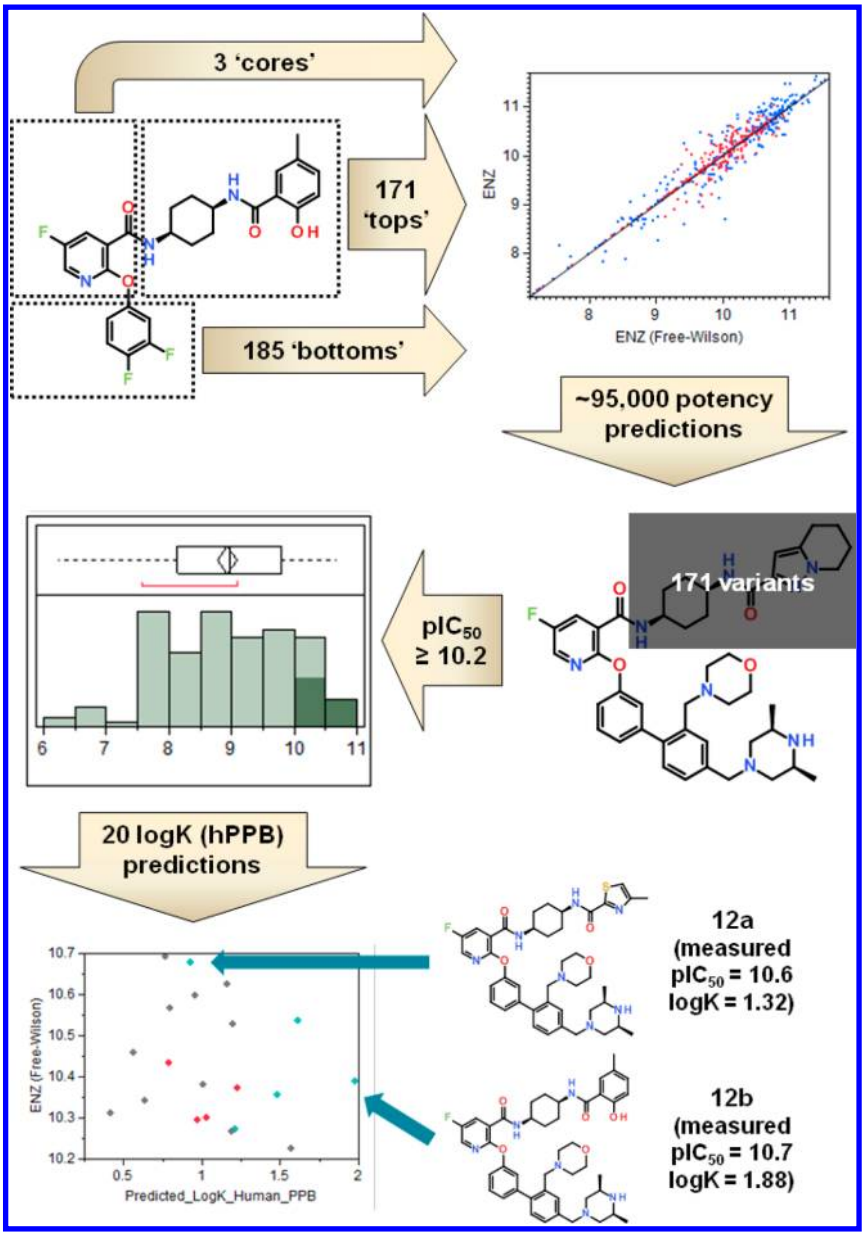

Figure 11. Multiparameter optimization of potency and plasma protein binding. (top left) Fragmentation scheme used for deconstruction of known actives. (top right) Free–Wilson model for enzyme pIC_{50} based on a combination of legacy (blue) and nonlegacy (red) series described in this paper. (center right) Substructure used to filter ~95000 potential fragment combinations down to 171. (center left) Histogram of predicted activities of these filtered compounds, highlighting those with predicted $pIC_{50} \geq 10.2$ in dark green. (bottom left) Scatter plot of predicted pIC_{50} vs predicted log *K* (log(bound fraction/free fraction)). Compounds that had been synthesized prior to the analysis are shown in red, virtual compounds not synthesized are gray, while those that were synthesized are shown in blue. The two most advanced compounds from these five are highlighted (bottom right).

Scheme 1[a]

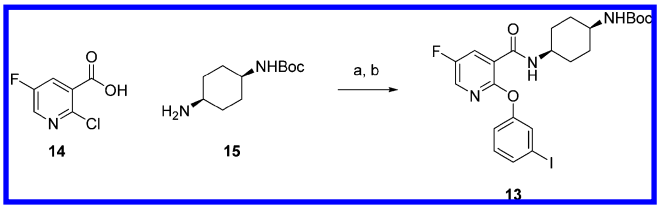

[a](a) T3P (1.57 M in THF), Et_3N, 0 °C to rt, MeCN, overnight, 98%; (b) 3-iodophenol, Cs_2CO_3, 60 °C, DMF, 48 h, 58%.

analogues bearing a hydroxyl on this ring (Scheme 4). Significantly higher yields were obtained if the Suzuki reaction was carried out using a bromoaryl aldehyde, compared to use of an aryl unit with the amine already in place (cf. use of **16** in Scheme 2).

Compounds with two or three methylene units between the aryl ring and the basic center could also be made from **13** by either route I or route II, but instead of reductive amination the base was most conveniently installed by using an appropriate alcohol, followed by mesylation and displacement (Scheme 5).

Synthesis of the dibasic compounds generally followed route II, with amidation as the final step. As the binding site tolerated only minor changes to the *ortho*-base with morpholine being preferred, the second aryl ring was most often added to the core structure with the morpholine in place. This then allowed parallel variation of the *para*-base and amide (Scheme 6).

dx.doi.org/10.1021/jm5001216 | J. Med. Chem. XXXX, XXX, XXX–XXX

Scheme 2[a]

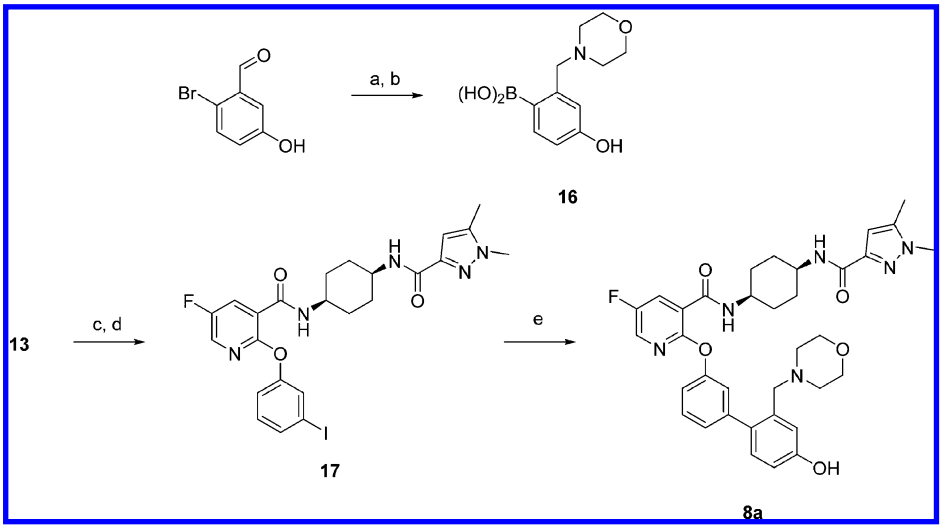

[a](a) Morpholine, $NaBH(OAc)_3$, CH_2Cl_2, 2 h; (b) *t*-BuLi, THF, −78 to 0 °C then $B(Oi\text{-}Pr)_3$, −78 °C to rt, 1 h, then NH_4Cl, H_2O, 2 h, 83% (2 steps); (c) 4 M HCl in 1,4-dioxane, CH_2Cl_2, 16 h, 100%; (d) 1,5-dimethyl-1*H*-pyrazole-3-carboxylic acid, T3P (1.57 M in THF), Et_3N, MeCN, 20 h, 97%; (e) **16**, SPhos, $Pd(OAc)_2$, K_2CO_3, 70 °C, H_2O, MeCN, 3 h, 9%.

Scheme 3[a]

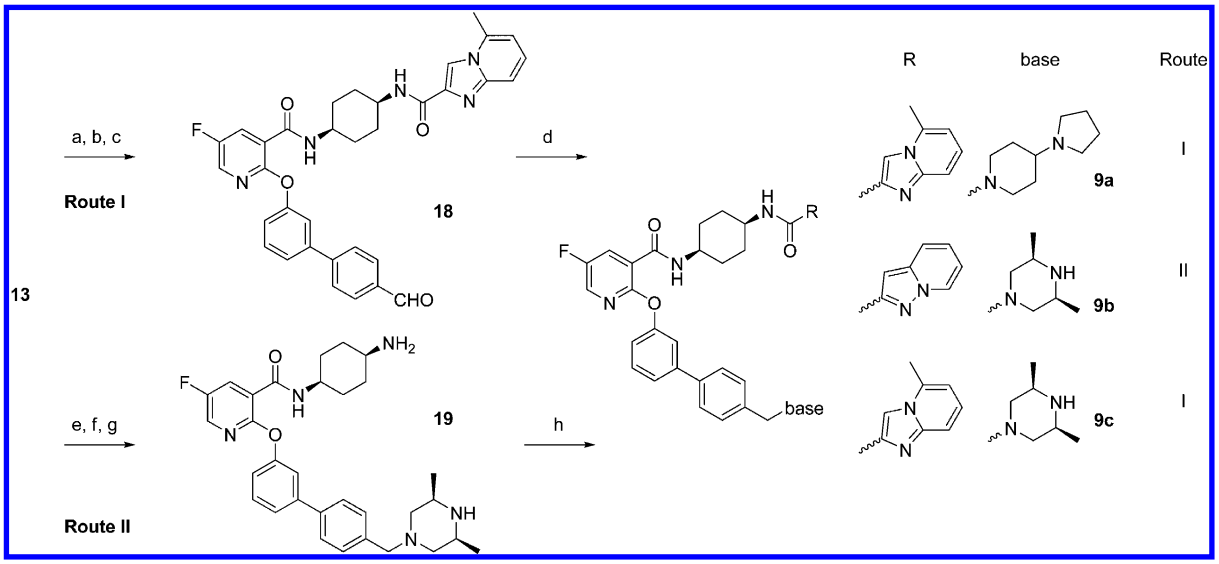

[a](a) 4 M HCl in 1,4-dioxane, CH_2Cl_2, 16 h, 100%; (b) 5-methylimidazo[1,2-*a*]pyridine-2-carboxylic acid, T3P (1.57 M in THF), Et_3N, MeCN, 20 h, 93%; (c) 4-formylphenylboronic acid, SPhos, $Pd(OAc)_2$, K_2CO_3, 80 °C, H_2O, MeCN, overnight, 86%; (d) amine, $NaBH(OAc)_3$, CH_2Cl_2, 1 h, 20−78%; (e) 4-formylphenylboronic acid, SPhos, $Pd(OAc)_2$, K_2CO_3, 70 °C, H_2O, MeCN, 1 h, 95%; (f) *cis*-2,6-dimethylpiperazine, $NaBH(OAc)_3$, CH_2Cl_2, 1 h, 95%; (g) 4 M HCl in 1,4-dioxane, CH_2Cl_2, 16 h, 100%; (h) appropriate acid, HATU, DIPEA, MeCN, 10 min, 20−50%. Final steps were not optimized and low yields were due to losses on HPLC purification. Compounds **10a** and **10c** were prepared in two steps from **17** (Scheme 2) using route I.

Identification of Preclinical Candidates. After profiling these *ortho*,*para*-dibasic compounds, two candidates, **12a** and **12b**, emerged, showing a range of superior properties including high cell potency, low unbound fraction in human PPB, and high in vitro turnover in human microsomes. Both compounds also had high solubility and could readily be crystallized to give stable crystalline solids with one predominant polymorph. Furthermore, the crystalline free base of **12b** was investigated further and shown to have good thermal properties (no thermal events below 80 °C) and low hygroscopicity (<2% at 25 °C and 80% relative humidity), making it suitable for micronization. Compounds **12a** and **12b** were highly selective for PDE4 over PDE1B, PDE2A, PDE3A, PDE5, PDE6, and PDE10A1 but showed little or no selectivity for PDE4B over PDE4D or PDE4A, or over the high-affinity rolipram binding site (HARBS). Both compounds were selected for in vivo profiling in rat lung inflammation and rat and dog pharmacokinetic studies (Table 7).

Compounds **12a** and **12b** significantly inhibited pulmonary inflammation with ED_{80} values of 0.02 and 0.06 mg/mL nebulizer concentration, respectively (Figure 12), which corresponded to a 0.2 and 0.6 μg/kg deposited dose in the lung based upon measured filter sample and terminal lung levels. In the duration experiment, both **12a** and **12b** inhibited LPS-induced pulmonary neutrophilia at 0.03 and 0.1 mg/mL nebulizer concentrations, respectively (Figure 13).

dx.doi.org/10.1021/jm5001216 | J. Med. Chem. XXXX, XXX, XXX−XXX

Scheme 4[a]

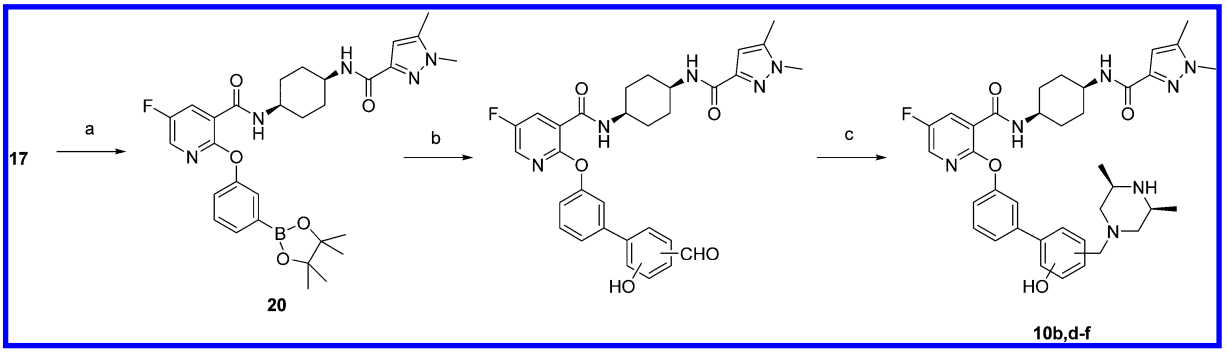

[a](a) Bis(pinacolato)diboron, (dppf)$PdCl_2$−CH_2Cl_2, dppf, KOAc, 80 °C, DMSO, 20 h, 86%; (b) bromo-hydroxybenzaldehyde, either $Pd(OAc)_2$, SPhos, K_2CO_3, 80 °C, H_2O, MeCN, 2 h, or $Pd(PPh_3)_4$, Na_2CO_3, reflux, H_2O, THF, overnight, 62-73%; (c) *cis*-2,6-dimethylpiperazine, $NaBH(OAc)_3$, CH_2Cl_2, 2 h, 25−41%. Final step was not optimized and low yields were due to losses on HPLC purification.

Scheme 5[a]

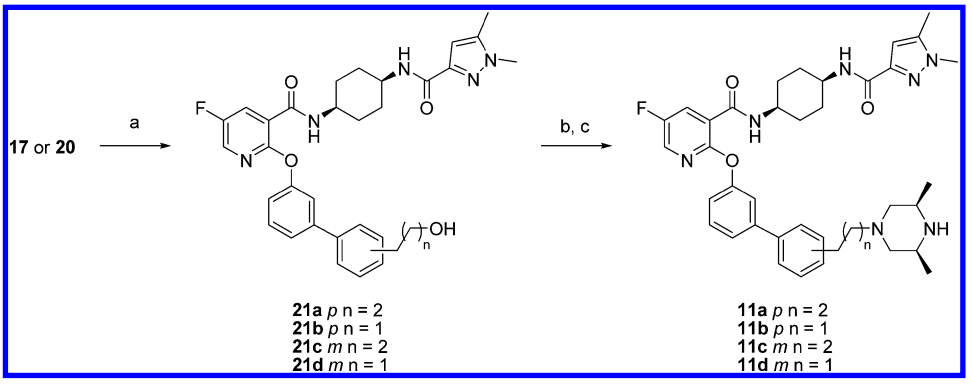

[a](a) For **21a**, **20**, 2-(4-bromophenyl)ethanol, for **21b−d**, **17**, hydroxyalkylphenylboronic acid, for **21a−d**, $Pd(PPh_3)_4$, Na_2CO_3, reflux, H_2O, THF, overnight, 65−83%; (b) MsCl, py, CH_2Cl_2, overnight, 76−97%; (c) *cis*-2,6-dimethylpiperazine, 80 °C, microwave, MeCN, 30 min, 35−57%. Final step was not optimized, and low yields were due to losses on HPLC purification. Compound **11e** was prepared from **21b** and 4-(pyrrolidin-1-yl)piperidine using the same conditions.

Scheme 6[a]

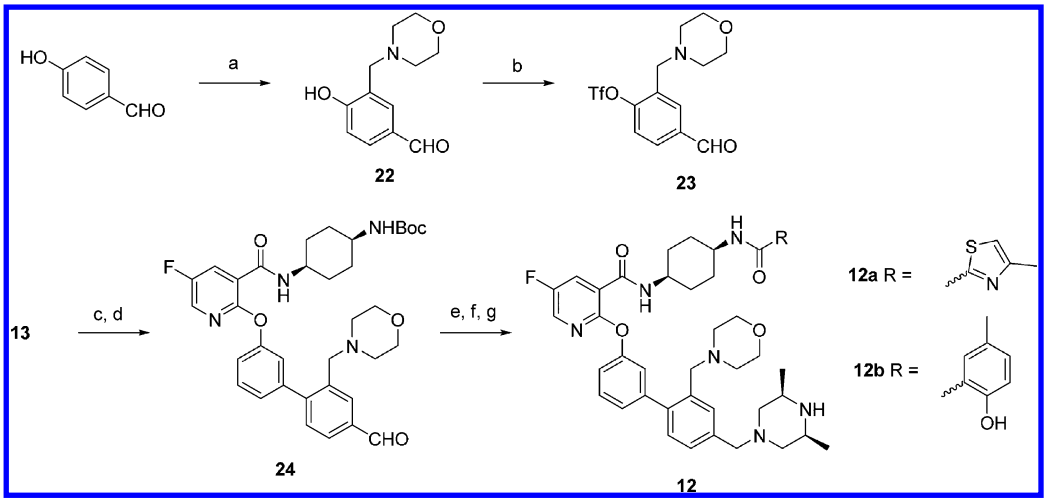

[a](a) HCHO, morpholine, 78 °C, EtOH, 11 h, 61%; (b) *N*-phenyltrifluoromethanesulfonimide, Et_3N, 0 °C to rt, CH_2Cl_2, 16 h, 95%; (c) bis(pinacolato)diboron, (dppf)$PdCl_2$−CH_2Cl_2, dppf, KOAc, 80 °C, DMSO, 16 h, 97%; (d) **23**, $Pd(OAc)_2$, SPhos, K_2CO_3, 70 °C, H_2O, MeCN, 2 h, 93%; (e) *cis*-2,6-dimethylpiperazine, $NaBH(OAc)_3$, AcOH, CH_2Cl_2, 20 h, 96%; (f) 4 M HCl in 1,4-dioxane, CH_2Cl_2, 1 h, 99%; (g) appropriate acid, EDCI, HOBt, Et_3N, THF, NMP, 20 h, 43−70%.

Compounds **12a** and **12b** showed moderate to high clearance in rat in vivo studies. The high terminal volumes of distribution (V_z) for these compounds can be explained by their dibasicity and lead to long half-lives. Compounds **12a** and **12b** were also dosed via the intratracheal route, showing similar half-lives in both plasma and lung; high concentrations were sustained in the

dx.doi.org/10.1021/jm5001216 | *J. Med. Chem.* XXXX, XXX, XXX−XXX

Table 7. Selected Properties of 12a and 12b Compared to 8a

property	8a	12a	12b
human PDE4B enzyme pIC_{50}[a]	10.8 (4)	10.6 (6)	10.7 (10)
human PDE4D enzyme pIC_{50}[a]	NT	10.7 (4)	10.7 (4)
human PDE4A1A enzyme pIC_{50}[a]	NT	>8.0 (1)	>8.0 (1)
HARBS pIC_{50}[a]	NT	>8.0 (1)	>8.0 (1)
rat PDE4B enzyme pIC_{50}[a]	NT	10.7 (4)	10.6 (6)
PBMC TNF-α pIC_{50}[a]	10.2 (4)	10.7 (2)	10.4 (12)
human whole blood TNF-α pIC_{50}[a]	NT	9.5 (4)	7.9 (10)
rat whole blood TNF-α pIC_{50}[a]	NT	NT	9.3 (2)
PPB %free human/rat[a]	5.6 (1)/10 (1)	4.5 (1)/23 (2)	1.3 (5)/8.3 (5)
aqueous solubility pH 7.4 (μM)[a]	250 (free base) (1)	>1400 (TFA salt) (1)	213 (free base) (3)
MW/clogP/log D[a]	643/3.4/3.1 (1)	756/6.0/1.9 (1)	765/7.1/2.8 (2)
human microsomal Cl_{int} (μL/min/mg)[a]	>150 (2)	>150 (1)	78 (1)
rat hepatocyte Cl_{int} (μL/min/10^6 cells)[a]	120 (2)	10 (9)	13 (9)
PDE selectivity[a,b]	NT	>10000× (1)	>10000× (1)
hERG binding pIC_{50}[a]	4.5 (2)	4.7 (2)	5.2 (2)
CYP inhibition pIC_{50} (8 isoforms)[a]	3A4 6.3, 2C9 6.6, 2C19 5.2, 2D6 <5 (1)	all <5.0 (1)	all <5.6 (1)
time dependent CYP inhibition[a]	73% inhibition at 50 μM (1)	none (1)	none (1)

	8a	12a		12b	
	rat	rat	dog	rat	dog
pharmacokinetics[c]					
Cl (mL/min/kg)	69	44	34	50	19
V_{dss}/V_z (L/kg)	2.6/76	18/27	26/44	16/30	13/25
iv $t_{1/2}$ (h)	13	7	15	7	15
F%	NT	NT	16	<16	6
i.t. $t_{1/2}$ (h)	NT	8		9	

	8a	12a	12b
in vivo efficacy			
LPS DRC; LENC[a]	0.1 mg/mL (1)	0.01 mg/mL (2)	0.01 mg/mL (2)
ED_{80} (nebulizer concentration/lung concentration/lung deposited dose)	ND	0.02 mg/mL/23 nM/0.2 μg/kg	0.06 mg/mL/78 nM/0.6 μg/kg
LPS duration; LENC[a]	0.1 mg/mL (1)	0.03 mg/mL (2)	0.1 mg/mL (2)

[a]Numbers of replicates are stated in brackets. [b]Tested against PDE1B, PDE2A, PDE3A, PDE5, PDE6, PDE10A1. [c]n = 2−3 animals.

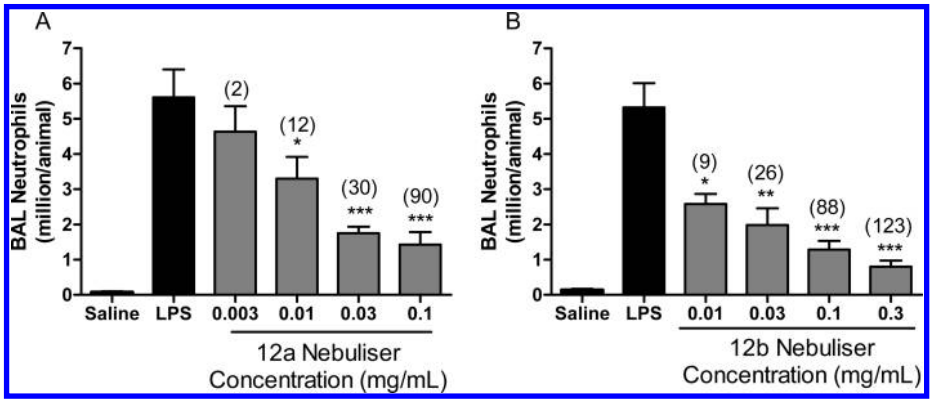

Figure 12. Effect of **12a** and **12b** on LPS-induced pulmonary neutrophilia in the rat. Both **12a** (A) and **12b** (B) inhibited LPS-induced neutrophilia in a dose-dependent manner (mg/mL nebulizer concentration) when administered by aerosol nose-only inhalation of a nebulized solution 30 min before LPS challenge. Brackets above bars signify measured terminal lung concentration (nM). n = 8 in all groups except n = 4 for saline group. Data representative from two separate experiments. *, **, *** = p < 0.05, 0.01, and 0.001 respectively.

lung while plasma concentrations were significantly lower, thereby offsetting the potential for any adverse side effects (Figure S4, Supporting Information). These compounds also showed low oral exposure and predictable $t_{1/2}$ in dog, consistent with the low fraction absorbed, high clearance, and V_z observed in the rat. Interestingly, there were no emetic episodes noted during either the iv or po PK studies in dog with **12b**. The dose equated to an iv $C_{max(free)}$ of 8 nM (iv dose 0.1 mg/kg), equating to a $C_{max(free)}$/PBMC potency ratio of 280, which gave confidence that emesis should not be an issue in the clinic for this compound.

A simple, pragmatic approach to predict human dose was to use the dose required to give 80% inhibition efficacy in the rat acute LPS challenge model and adjust for human−rat differences in the PDE4 binding potency. As the estimated lung delivered

dx.doi.org/10.1021/jm5001216 | J. Med. Chem. XXXX, XXX, XXX−XXX

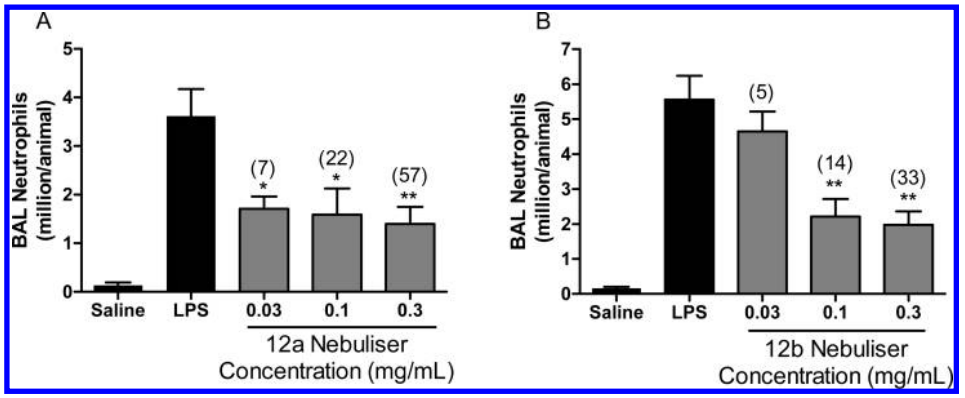

Figure 13. Effect of **12a** and **12b** when dosed 12 h before LPS exposure in the rat. Both **12a** (A) and **12b** (B) inhibited LPS-induced neutrophilia when administered by aerosol nose-only inhalation of a nebulized solution 12 h before LPS challenge (mg/mL nebulizer concentration). Brackets above bars signify measured terminal lung concentration (nM). $n = 8$ in all groups except $n = 4$ for saline group. Data representative from two separate experiments. *, **, *** = $p < 0.05$, 0.01, and 0.001, respectively.

doses for **12b** and **12a** were 0.6 and 0.2 μg/kg, respectively, and PDE4 potencies in rat and human were equivalent, the expected human doses for compounds **12b** and **12a** were predicted to be 0.6 and 0.2 μg/kg, respectively (Table 8). A complementary yet more robust approach was to predict the human dose from a multicompartment PK model (using a nonlinear regression model in WinNonlin) as described previously.[30] This model represents blood, tissues, and a "deep compartment", hypothesized to consist of specific tissues having higher affinity for dibasic compounds, perhaps in organelles such as lysosomes. It was speculated that the terminal half-lives were controlled largely by the rate of diffusion of compounds from this deep compartment back into blood. A range of reference compounds were dosed to rat via both iv and *i.t.* routes, and iv route in dog, and both plasma and lung measurements were made over time. Furthermore, both plasma and lung measurements were determined after inhalation dosing in rat. The lung and plasma concentration−time PK data for **12a** and **12b** were fitted to this five-compartmental model which described the profiles well. The therapeutic human dose was estimated from the predicted lung concentration at the end of the dosing interval. This was possible because it was known what lung concentration was required for 80% efficacy in the rat acute LPS model. The ED_{80}s were calculated at 0.02 and 0.06 mg/mL nebulizer concentrations respectively for **12a** and **12b**, which gave total lung concentrations of 23 and 78 nM, and it can be assumed that the same lung concentration in man will give equivalent efficacy. Clearance was estimated to be 9 and 3 mL/min/kg (Figure S5, Supporting Information), plasma fraction unbound was measured as 0.045 and 0.013, and physiological lung volume was taken to be 8 mL/kg. This simulation estimated an efficacious human lung deposited dose of 1 μg/kg for both compounds, which was comparable to the lung dose required in the rat LPS model. The total $C_{max,ss}$ were also comparable to the values estimated from the correlation between dose and C_{max} with other marketed inhaled therapies (Figures S6 and S7, Supporting Information).[20] Finally the simulated human terminal lung half-lives were consistent with these compounds being suitable for once daily dosing.

Table 8. Predicted Human Pharmacokinetics for 12a and 12b

parameter	12a	12b
human total clearance (mL/min/kg)	9	3
human $t_{1/2}$ (h)	14	10
lung delivered dose predicted from the rat LPS model after adjusting for species differences in potency (μg/kg)	0.2	0.6
predicted lung delivered dose using PK modeling method (μg/kg)	1	1

Experiments to investigate the emetic profile of **12b** were undertaken in ferrets.[31] The compound was administered by iv infusion (0.3, 1, and 3 mg/kg), then the animals were observed for incidence of emetic episodes, salivation, and behavioral changes. **12b** shows a 625× free plasma/PBMC ratio at the non-nauseous dose of 0.3 mg/kg. At doses which produced retching in 50% of the animals, the ratio of free plasma/PBMC potency was 243× higher for **12b** compared to **2**, demonstrating that **12b** has a much lower emetic potential. Given that the predicted efficacious human inhaled dose for **12b** is so low, it is highly unlikely that this compound would cause emesis in the clinic.

CONCLUSIONS

We have reported a lead optimization campaign that has led to the discovery of novel and highly potent inhaled PDE4 inhibitors. Combining both learnings and shortcomings from the medicinal chemistry properties associated with **4** and our own historical series, a general method to confidently predict whether a compound would show efficacy and duration in our in-house efficacy experiment was developed using nominal logistic regression. Toward the end of the lead optimization process, a Free−Wilson model was built for PDE4 potency and a large virtual library of compounds were proposed. Compounds were prioritized using this model and human protein binding predictions and a focused synthesis campaign led to compounds **12a** and **12b**. These both showed striking anti-inflammatory efficacy when administered by inhalation to rats as aqueous solutions either 30 min or up to 12 h before LPS challenge. They showed sustained duration of action in these in-house models which was superior to that of **4** and **5**. Compound **12b** had a very low predicted efficacious human inhaled dose of 1 μg/kg and would be highly unlikely to cause emesis in the clinic due to its very high ratio of free plasma/PBMC potency compared to cilomilast in ferret emesis experiments. Compounds **12a** and **12b** thus serve as interesting preclinical compounds for the treatment of COPD.

EXPERIMENTAL SECTION

Reagents were obtained from commercial suppliers and used without purification. Unless otherwise stated, reactions were carried out at

dx.doi.org/10.1021/jm5001216 | J. Med. Chem. XXXX, XXX, XXX−XXX

ambient temperature (18−25 °C) and under positive nitrogen pressure with magnetic stirring. Flash chromatography was performed on E. Merck 230−400 mesh silica gel 60 or by using Biotage KP-Sil SNAP cartridges. Solvent mixtures used as eluents are volume/volume ratios. Preparative HPLC purifications were performed on Waters Symmetry, Novapak, or XTerra columns eluting with a gradient of acetonitrile or methanol in aqueous ammonium acetate, ammonia, or trifluoroacetic acid solution. Routine ^{1}H NMR spectra were recorded on a Varian UnityInova spectrometer at a proton frequency of 300 or 400 MHz or a Bruker Avance III spectrometer at a proton frequency of 500 MHz. Chemical shifts are expressed in ppm. Mass spectra were measured on an Agilent 1100 MSD G1946D spectrometer using electrospray ionization, atmospheric pressure chemical ionization, or Agilent Multimode ionization; only ions that indicate the parent mass are reported. The purity of all test compounds was determined by RP HPLC conducted on an Agilent 1100 LC/MS system, using UV detection and a gradient of 5−95% acetonitrile in either aqueous ammonium acetate (0.1% w/v) or trifluoroacetic acid (0.1% v/v) over 2.5 min on 2.1 mm × 5 mm columns packed with Waters Symmetry C8 or Waters Symmetry C18, or 2.0 mm × 50 mm columns packed with Phenomenex Max-RP. All test compounds were ≥95% purity.

***tert*-Butyl (1s,4s)-4-(2-Chloro-5-fluoronicotinamido)-cyclohexylcarbamate 25.** 2-Chloro-5-fluoronicotinic acid **14** (16.5 g, 1 equiv) and *tert*-butyl (1*s*,4*s*)-4-aminocyclohexylcarbamate **15** (25.2 g, 1.25 equiv) were suspended in MeCN (550 mL), then Et_3N (78 mL, 6 equiv) was added. The stirred mixture was cooled in ice while T3P (1.57 M in THF, 78 mL, 1.3 equiv) was slowly added. The reaction became homogeneous and was allowed to slowly warm to rt overnight. All volatiles were evaporated, and the residue was partitioned between aqueous 2 M HCl and EtOAc. The aqueous phase was separated and extracted into further EtOAc (×2). The combined organic solutions were washed with water, saturated aqueous $NaHCO_3$, and brine. The organic layer was dried ($MgSO_4$) and concentrated to give **25** as a cream-colored foam (34.2 g, 98%). ^{1}H NMR (400 MHz, $CDCl_3$, δ): 8.34 (d, J = 2.8 Hz, 1H), 7.92 (dd, J = 7.9, 3.1 Hz, 1H), 6.70 (d, J = 6.7 Hz, 1H), 4.56 (d, J = 6.4 Hz, 1H), 4.21−4.12 (m, 1H), 3.71−3.57 (m, 1H), 1.92−1.80 (m, 4H), 1.79−1.70 (m, 2H), 1.64−1.50 (m, 2H), 1.45 (s, 9H).

***tert*-Butyl (1s,4s)-4-(5-Fluoro-2-(3-iodophenoxy)-nicotinamido)cyclohexylcarbamate 13.** A mixture of **25** (11.31 g, 1 equiv), 3-iodophenol (6.69 g, 1 equiv), and Cs_2CO_3 (19.82 g, 2 equiv) was heated at 60 °C in DMF (150 mL) for 48 h then poured onto water (300 mL). The resulting solid was removed by filtration and dissolved in EtOAc, which was washed with aqueous 2 M HCl, water, and brine. The organic layer was dried (Na_2SO_4) and concentrated to give crude product, which was purified by flash silica chromatography, elution gradient 30−40% EtOAc in isohexane, to give **13** as a white foam (9.80 g, 58%). ^{1}H NMR (300 MHz, $CDCl_3$, δ): 8.35 (dd, J = 8.2, 3.2 Hz, 1H), 8.06 (d, J = 3.3 Hz, 1H), 7.84 (d, J = 7.1 Hz, 1H), 7.65 (dt, J = 7.6, 1.4 Hz, 1H), 7.53 (t, J = 1.7 Hz, 1H), 7.23−7.11 (m, 2H), 4.41 (s, 1H), 4.21−4.10 (m, 1H), 3.59−3.67 (m, 1H), 1.87−1.75 (m, 6H), 1.75−1.62 (m, 2H), 1.44 (s, 9H).

4-Hydroxy-2-(morpholinomethyl)phenylboronic Acid 16. Morpholine (1.19 mL, 1.1 equiv) was added to a solution of 2-bromo-5-hydroxybenzaldehyde (2.50 g, 1 equiv) in CH_2Cl_2 (20 mL) and stirred for 20 min. Sodium triacetoxyborohydride (2.90 g, 1.1 equiv) was added and stirred for 2 h. The reaction was quenched with MeOH and stirred for 1 h. The solution was concentrated, dissolved in MeOH, and loaded onto a SCX (50 g) column, flushing with MeOH. Eluting with methanolic ammonia and concentration of the eluent gave 4-bromo-3-(morpholinomethyl)phenol (3.0 g, 89%), which was dissolved in THF (60 mL) and cooled to −78 °C, then 1.7 M *t*-butyllithium (19.45 mL, 3 equiv) was added dropwise. The reaction mixture was stirred for 10 min then warmed to 0 °C for 15 min. The reaction was then cooled to −78 °C and triisopropyl borate (7.6 mL, 3 equiv) added. The reaction was warmed to rt and stirred for 1 h. Saturated aqueous NH_4Cl was added and the reaction stirred at rt for 2 h. The reaction mixture was diluted with EtOAc (200 mL), the phases were separated, and the aqueous was further extracted with EtOAc. The combined organic extracts were washed with saturated brine, dried ($MgSO_4$), and concentrated to give **16** (2.45 g, 83% over 2 steps). LRMS: m/z 238 $[M + H]^+$.

***N*-((1s,4s)-4-Aminocyclohexyl)-5-fluoro-2-(3-iodophenoxy)-nicotinamide 26 [General Method A].** To a solution of **13** (3.10 g, 1 equiv) in CH_2Cl_2 (30 mL) was added 4 M HCl in 1,4-dioxane (20 mL, 14 equiv). The mixture was stirred at rt overnight then concentrated to dryness to give **26** hydrochloride as a white solid (2.74 g, 100%). ^{1}H NMR (400 MHz, CD_3OD, δ): 8.10 (d, J = 3.1 Hz, 1H), 8.02 (dd, J = 7.9, 3.1 Hz, 1H), 7.61−7.57 (m, 2H), 7.19−7.17 (m, 2H), 4.13−4.08 (m, 1H), 3.27−3.22 (m, 1H), 1.97−1.65 (m, 8H). This compound could also be used as the free base after neutralization and extraction into CH_2Cl_2.

***N*-((1s,4s)-4-(1,5-Dimethyl-1*H*-pyrazole-3-carboxamido)-cyclohexyl)-5-fluoro-2-(3-iodophenoxy)nicotinamide 17 [General Method B].** T3P (1.57 M in THF, 5.2 mL, 1.1 equiv) was added to a stirred solution of **26** (3.50 g, 1 equiv), 1,5-dimethyl-1*H*-pyrazole-3-carboxylic acid (1.10 g, 1.1 equiv), and Et_3N (9.9 mL, 10 equiv) in MeCN (20 mL) and stirred at rt for 20 h. The mixture was concentrated, dissolved in EtOAc, washed with saturated aqueous $NaHCO_3$, water, and brine, dried ($MgSO_4$), and concentrated to give **17** as a white solid (4.00 g, 97%). ^{1}H NMR (400 MHz, $CDCl_3$, δ): 8.36 (dd, J = 8.2, 3.1 Hz, 1H), 8.07 (d, J = 3.1 Hz, 1H), 7.87 (d, J = 6.7 Hz, 1H), 7.64 (dt, J = 7.5, 1.5 Hz, 1H), 7.55 (t, J = 1.8 Hz, 1H), 7.22−7.14 (m, 2H), 6.69 (d, J = 7.7 Hz, 1H), 6.53 (s, 1H), 4.26−4.17 (m, 1H), 4.12−4.03 (m, 1H), 3.78 (s, 3H), 2.28 (s, 3H), 1.95−1.73 (m, 6H), 1.67−1.58 (m, 2H).

***N*-((1s,4s)-4-(1,5-Dimethyl-1*H*-pyrazole-3-carboxamido)-cyclohexyl)-5-fluoro-2-(4′-hydroxy-2′-(morpholinomethyl)-biphenyl-3-yloxy)nicotinamide 8a.** To a solution of SPhos (28 mg, 0.2 equiv) in MeCN (15 mL) was added $Pd(OAc)_2$ (8 mg, 0.1 equiv). The mixture was stirred for 10 min at rt before a solution of K_2CO_3 (0.144 g, 3 equiv) in water (5 mL) was added, followed by **17** (0.200 g, 1 equiv) and **16** (82 mg, 1 equiv). The mixture was heated at 70 °C for 3 h then poured into water and extracted into EtOAc, and the crude product was purified by preparative HPLC to give **8a** as a solid (21 mg, 9%). ^{1}H NMR (400 MHz, $CDCl_3$, δ): 8.33 (dd, J = 7.9, 3.1 Hz, 1H), 8.05 (d, J = 3.1 Hz, 1H), 8.02 (d, J = 7.2 Hz, 1H), 7.55 (t, J = 7.9 Hz, 1H), 7.31 (s, 1H), 7.23−7.18 (m, 3H), 7.14 (d, J = 7.7 Hz, 1H), 7.10 (t, J = 1.8 Hz, 1H), 6.90 (dd, J = 8.5, 2.1 Hz, 1H), 6.51 (s, 1H), 4.30 (s, 2H), 4.24−4.19 (m, 1H), 4.06−4.00 (m, 1H), 3.83−3.77 (m, 4H), 3.73 (s, 3H), 3.22−2.72 (m, 4H), 2.29 (s, 3H), 1.94−1.79 (m, 6H), 1.71−1.62 (m, 2H). LRMS: m/z 643 $[M + H]^+$.

***tert*-Butyl (1s,4s)-4-(5-Fluoro-2-(4′-formylbiphenyl-3-yloxy)-nicotinamido)cyclohexylcarbamate 27 [General Method C].** A solution of K_2CO_3 (1.64 g, 3 equiv) in water (15 mL), **13** (2.20 g, 3 equiv), and 4-formylphenylboronic acid (0.713 g, 1.2 equiv) were added sequentially to a stirred solution of $Pd(OAc)_2$ (89 mg, 0.1 equiv) and SPhos (0.319 g, 0.2 equiv) in MeCN (20 mL) then heated at 70 °C for 1 h. The mixture was cooled to rt, extracted with EtOAc, washed with water and brine, dried ($MgSO_4$), and concentrated. The residue was purified by flash silica chromatography, eluting with 40% EtOAc in isohexane to give **27** (2.00 g, 95%). ^{1}H NMR (300 MHz, $CDCl_3$, δ): 10.01 (s, 1H), 8.33 (dd, J = 7.9, 3.3 Hz, 1H), 8.03 (d, J = 3.3 Hz, 1H), 7.92 (d, J = 7.9 Hz, 2H), 7.73 (d, J = 7.9 Hz, 2H), 7.55 (d, J = 5.3 Hz, 2H), 7.41 (s, 1H), 7.18 (m, 1H), 4.48 (m, 1H), 4.16 (m, 1H), 3.58 (m, 1H), 1.75 (m, 6H), 1.50 (m, 2H), 1.36 (s, 9H).

***tert*-Butyl (1s,4s)-4-(2-(4′-(((3*S*,5*R*)-3,5-Dimethylpiperazin-1-yl)methyl)biphenyl-3-yloxy)-5-fluoronicotinamido)-cyclohexylcarbamate 28 [General Method D].** To a solution of **27** (0.780 g, 1 equiv) in CH_2Cl_2 (5 mL) was added *cis*-2,6-dimethylpiperazine (0.250 g, 1.5 equiv). The mixture was allowed to stir at rt for 2 h, then sodium triacetoxyborohydride (0.465 g, 1.5 equiv) was added. After stirring for 1 h, the mixture was diluted with CH_2Cl_2 and washed with saturated aqueous $NaHCO_3$, dried ($MgSO_4$), and concentrated to give **28** as a foam (0.880 g, 95%). ^{1}H NMR (300 MHz, $CDCl_3$, δ): 8.37 (dd, J = 7.8, 3.1 Hz, 1H), 8.08−8.03 (m, 2H), 7.56−7.53 (m, 4H), 7.42−7.35 (m, 3H), 7.15−7.10 (m, 1H), 4.38−4.31 (m, 1H), 4.22−4.14 (m, 1H), 3.65−3.57 (m, 1H), 3.54 (s, 2H), 3.00−2.93 (m, 2H), 2.82−2.75 (m, 2H), 1.85−1.61 (m, 10H), 1.41 (s, 9H), 1.04 (d, J = 6.4 Hz, 6H).

***tert*-Butyl (1s,4s)-4-(5-Fluoro-2-(3-(4,4,5,5-tetramethyl-1,3,2-dioxaborolan-2-yl)phenoxy)nicotinamido)cyclohexylcarbamate 29 [General Method E].** $PdCl_2(dppf)CH_2Cl_2$ (0.129 g, 0.05 equiv) and dppf (88 mg, 0.05 equiv) were stirred together in dry DMSO

dx.doi.org/10.1021/jm5001216 | J. Med. Chem. XXXX, XXX, XXX−XXX

(4 mL) for 10 min, then KOAc (0.927 g, 3 equiv), a solution of **13** (1.748 g, 1 equiv) in DMSO (8 mL), and bis(pinacolato)diboron (1.063 g, 1.3 equiv) were added and the reaction mixture heated at 80 °C for 16 h. After cooling to rt, water (10 mL) was added and the mixture stirred for 3 h. The solid was removed by filtration and washed with water (2 × 10 mL) then purified by flash silica chromatography, elution gradient 60−100% EtOAc in isohexane to give **29** as a pale-brown oil (1.704 g, 97%). ^{1}H NMR (400 MHz, $CDCl_3$, δ): 8.35 (dd, J = 8.2, 3.1 Hz, 1H), 8.06−8.03 (m, 2H), 7.76 (d, J = 7.4 Hz, 1H), 7.56 (d, J = 2.6 Hz, 1H), 7.49 (t, J = 7.7 Hz, 1H), 7.28−7.25 (m, 1H), 4.44−4.38 (m, 1H), 4.19−4.14 (m, 1H), 3.65−3.59 (m, 1H), 1.87−1.36 (m, 8H), 1.42 (s, 9H), 1.35 (s, 12H).

***N*-((1s,4s)-4-(1,5-Dimethyl-1*H*-pyrazole-3-carboxamido)-cyclohexyl)-5-fluoro-2-(3-(4,4,5,5-tetramethyl-1,3,2-dioxaborolan-2-yl)phenoxy)nicotinamide 20.** Prepared from **17** using general method E, in 86% yield. ^{1}H NMR (400 MHz, $CDCl_3$, δ): 8.36 (dd, J = 8.3, 3.2 Hz, 1H), 8.10−8.04 (m, 2H), 7.74 (dd, J = 6.4, 1.0 Hz, 1H), 7.56 (d, J = 2.3 Hz, 1H), 7.49 (t, J = 7.8 Hz, 1H), 7.29 (ddd, J = 8.1, 2.5, 1.1 Hz, 1H), 6.65 (d, J = 7.4 Hz, 1H), 6.51 (s, 1H), 4.26−4.17 (m, 1H), 4.11−4.03 (m, 1H), 3.75 (s, 3H), 2.27 (s, 3H), 1.94−1.73 (m, 6H), 1.67−1.56 (m, 2H), 1.32 (s, 12H).

***N*-((1s,4s)-4-(1,5-Dimethyl-1*H*-pyrazole-3-carboxamido)-cyclohexyl)-5-fluoro-2-(4′-(3-hydroxypropyl)biphenyl-3-yloxy)nicotinamide 21a [General Method F].** $Pd(PPh_3)_4$ (24 mg, 0.02 equiv) was added to a mixture of **17** (0.600 g, 1 equiv), 4-(3-hydroxypropyl)phenylboronic acid (0.224 g, 1.2 equiv), and Na_2CO_3 (0.330 g, 3 equiv) in water (2.5 mL) and THF (5 mL). The mixture was heated at 70 °C for 18 h, then allowed to cool, diluted with EtOAc, and washed with water and brine. The organic layer was dried (Na_2SO_4) and concentrated to give crude product which was purified by flash silica chromatography, eluting with 0−5% MeOH in EtOAc to give **21a** as a white foam (0.480 g, 79%). ^{1}H NMR (400 MHz, CD_3OD, δ): 8.37 (dd, J = 8.2, 3.1 Hz, 1H), 8.11−8.05 (m, 2H), 7.55−7.47 (m, 4H), 7.37−7.35 (m, 1H), 7.25−7.22 (m, 2H), 7.16−7.12 (m, 1H), 6.67 (d, J = 7.7 Hz, 1H), 6.50 (s, 1H), 4.27−4.19 (m, 1H), 4.12−4.01 (m, 1H), 3.70 (t, J = 6.3 Hz, 2H), 3.66 (s, 3H), 2.74 (t, J = 7.8 Hz, 2H), 2.25 (s, 3H) 1.95−1.75 (m, 6H), 1.67−1.54 (m, 4H).

***N*-((1s,4s)-4-(1,5-Dimethyl-1*H*-pyrazole-3-carboxamido)-cyclohexyl)-2-(4′-(3-((3*S*,5*R*)-3,5-dimethylpiperazin-1-yl)-propyl)biphenyl-3-yloxy)-5-fluoronicotinamide 11a [General Method G].** To a solution of **21a** (0.610 g, 1 equiv) and pyridine (0.30 mL, 3.5 equiv) in CH_2Cl_2 (7 mL) was added mesyl chloride (0.28 mL, 3.5 equiv) and the reaction stirred at rt overnight. The reaction mixture was concentrated to give a residue which was partitioned between EtOAc and aqueous 2 M HCl. The organic layer was washed with further 2 M HCl, saturated aqueous $NaHCO_3$, and brine, dried ($MgSO_4$), and concentrated to give a yellow oil. This was triturated with ether to give the methanesulfonate as a white solid (0.665 g, 96%). The methanesulfonate (0.145 g, 1 equiv) was added to a microwave tube with *cis*-2,6-dimethylpiperazine (75 mg, 3 equiv) and MeCN (1 mL). The reaction was microwaved at 80 °C for 30 min. The crude product was purified by preparative HPLC to give **11a** trifluoroacetic acid salt as a white solid (86 mg, 43%). ^{1}H NMR (400 MHz, CD_3OD, δ): 8.13−8.07 (m, 1H), 8.04 (d, J = 7.9 Hz, 1H), 7.54−7.36 (m, 5H), 7.24 (d, J = 7.2 Hz, 2H), 7.18−7.09 (m, 1H), 6.43 (s, 1H), 4.13−4.05 (m, 1H), 3.97−3.87 (m, 1H), 3.75−3.55 (m, 7H), 3.11−2.98 (m, 2H), 2.90−2.76 (m, 2H), 2.77−2.65 (m, 2H), 2.24 (s, 3H), 2.10−1.97 (m, 2H), 1.91−1.59 (m, 8H), 1.35 (d, J = 6.0 Hz, 6H). LRMS: m/z 682 $[M + H]^+$.

***N*-((1s,4s)-4-(1,5-Dimethyl-1*H*-pyrazole-3-carboxamido)-cyclohexyl)-5-fluoro-2-(4′-(2-hydroxyethyl)biphenyl-3-yloxy)-nicotinamide 21b.** Prepared from **20** and 2-(4-bromophenyl)ethanol using general method F, in 70% yield. ^{1}H NMR (400 MHz, $CDCl_3$, δ): 8.38 (dd, J = 8.2, 3.1 Hz, 1H), 8.08 (d, J = 3.1 Hz, 1H), 8.06 (s, 1H), 7.56−7.48 (m, 4H), 7.38−7.34 (m, 1H), 7.29−7.26 (m, 2H), 7.17−7.13 (m, 1H), 6.67 (d, J = 7.5 Hz, 1H), 6.50 (s, 1H), 4.27−4.19 (m, 1H), 4.12−4.01 (m, 1H), 3.94−3.86 (m, 2H), 3.67 (s, 3H), 2.90 (t, J = 6.5 Hz, 2H), 2.25 (s, 3H), 1.96−1.75 (m, 6H), 1.68−1.57 (m, 2H).

***N*-((1s,4s)-4-(1,5-Dimethyl-1*H*-pyrazole-3-carboxamido)-cyclohexyl)-5-fluoro-2-(4′-(2-(4-(pyrrolidin-1-yl)piperidin-1-yl)-ethyl)biphenyl-3-yloxy)nicotinamide 11e.** Prepared from **21b** and 4-(pyrrolidin-1-yl)piperidine via the intermediate methanesulfonate using general method G, as the trifluoroacetic acid salt in 30% yield over 2 steps. ^{1}H NMR (400 MHz, DMSO-d_6, 90 °C, δ): 8.21 (d, J = 3.1 Hz, 1H), 8.12−8.07 (m, 1H), 8.03−7.95 (m, 1H), 7.63−7.55 (m, 2H), 7.51−7.44 (m, 2H), 7.44−7.40 (m, 1H), 7.32 (d, J = 8.2 Hz, 2H), 7.22−7.14 (m, 1H), 6.97 (d, J = 7.7 Hz, 1H), 6.38−6.33 (m, 1H), 4.03−3.95 (m, 1H), 3.88−3.77 (m, 1H), 3.70 (s, 3H), 3.58−3.08 (m, 11H), 3.02−2.91 (m, 2H), 2.91−2.70 (m, 2H), 2.24 (s, 3H), 2.02−1.61 (m, 14H). LRMS: m/z 708 $[M + H]^+$.

4-Hydroxy-3-(morpholinomethyl)benzaldehyde 22. 4-Hydroxybenzaldehyde (10.0 g, 1 equiv) was dissolved in ethanol (100 mL) and formaldehyde (37% in water, 6.1 mL, 1 equiv) added, followed by morpholine (7.1 mL, 1 equiv). The reaction mixture was heated at 78 °C for 6 h, left at rt overnight, then further additions of 37% aqueous formaldehyde and morpholine (0.5 eq of each) were made and the mixture heated at 78 °C for 5 h. The mixture was concentrated and the residue purified by flash silica chromatography, elution gradient 20−50% EtOAc (containing 2% Et_3N and 2% MeOH) in isohexane to give **22** as a colorless oil (11.00 g, 61%). ^{1}H NMR (500 MHz, $CDCl_3$, δ): 9.82 (s, 1H), 7.72 (dd, J = 8.3, 1.9 Hz, 1H), 7.58 (s, 1H), 6.93 (d, J = 8.3 Hz, 1H), 3.85−3.70 (m, 4H), 3.80 (s, 2H), 2.70−2.50 (m, 4H).

4-Formyl-2-(morpholinomethyl)phenyl Trifluoromethanesulfonate 23. *N*-Phenyltrifluoromethanesulfonimide (5.09 g, 1.5 equiv) was added to an ice-cooled solution of **22** (2.10 g, 1 equiv) and Et_3N (4 mL, 3 equiv) in CH_2Cl_2 (20 mL). The mixture was allowed to warm to rt and stirred for a further 16 h. The solution was washed with water and brine, dried (Na_2SO_4), and concentrated. The residue was purified by flash silica chromatography eluting with 30% EtOAc in isohexane to give **23** as a colorless oil (3.17 g, 95%). ^{1}H NMR (400 MHz, $CDCl_3$, δ): 10.05 (s, 1H), 8.02 (d, J = 2.2 Hz, 1H), 7.90 (dd, J = 8.3, 2.2 Hz, 1H), 7.44 (d, J = 8.4 Hz, 1H), 3.74−3.68 (m, 4H), 3.62 (s, 2H), 2.51−2.42 (m, 4H).

***tert*-Butyl (1s,4s)-4-(5-Fluoro-2-(4′-formyl-2′-(morpholinomethyl)-biphenyl-3-yloxy)nicotinamido)cyclohexylcarbamate 24.** A solution of K_2CO_3 (0.396 g, 3 equiv) in water (3 mL), **23** (0.405 g, 1.2 equiv) and **29** (0.530 g, 1 equiv) were added sequentially to a stirred solution of $Pd(OAc)_2$ (21 mg, 0.1 equiv) and SPhos (78 mg, 0.2 equiv) in MeCN (5 mL). The mixture was heated at 70 °C for 2 h then cooled to rt, extracted with EtOAc, washed with water and brine, dried ($MgSO_4$), and concentrated. The residue was purified by flash silica chromatography eluting with 30% EtOAc in isohexane to give **24** as a brown foam (0.560 g, 93%). ^{1}H NMR (400 MHz, $CDCl_3$, δ): 10.07 (s, 1H), 8.37 (dd, J = 8.2, 3.1 Hz, 1H), 8.06 (d, J = 3.1 Hz, 1H), 8.01 (d, J = 1.5 Hz, 1H), 7.96 (d, J = 7.3 Hz, 1H), 7.85 (dd, J = 7.8, 1.7 Hz, 1H), 7.59−7.46 (m, 2H), 7.36 (d, J = 7.8 Hz, 1H), 7.32−7.29 (m, 1H), 7.23−7.17 (m, 1H), 4.56−4.41 (m, 1H), 4.22−4.13 (m, 1H), 3.67−3.60 (m, 1H), 3.60−3.55 (m, 4H), 3.49 (s, 2H), 2.41−2.30 (m, 4H), 1.89−1.47 (m, 8H), 1.43 (s, 9H).

***tert*-Butyl (1s,4s)-4-(2-(4′-(((3*S*,5*R*)-3,5-Dimethylpiperazin-1-yl)methyl)-2′-(morpholinomethyl)biphenyl-3-yloxy)-5-fluoronicotinamido)cyclohexylcarbamate 30.** **24** (0.280 g, 1 equiv) and *cis*-2,6-dimethylpiperazine (51 mg, 1 equiv) were stirred in CH_2Cl_2 (10 mL) for 15 min. AcOH (51 μL, 2 equiv) was added, followed by sodium triacetoxyborohydride (0.188 g, 2 equiv), and the reaction stirred for a further 20 h. The reaction was quenched with aqueous 2 M HCl, extracted with EtOAc, washed with water and brine, dried (Na_2SO_4), and concentrated to give **30** as a light-brown foam (0.310 g, 96%). ^{1}H NMR (300 MHz, $CDCl_3$, δ): 8.36 (dd, J = 8.2, 3.1 Hz, 1H), 8.06 (d, J = 3.2 Hz, 1H), 8.02 (d, J = 7.5 Hz, 1H), 7.50 (t, J = 7.9 Hz, 1H), 7.40−7.27 (m, 5H), 7.19−7.11 (m, 1H), 4.57−4.41 (m, 1H), 4.23−4.10 (m, 1H), 3.68−3.59 (m, 1H), 3.59−3.50 (m, 6H), 3.42 (s, 2H), 3.09−2.95 (m, 2H), 2.74−2.85 (m, 2H), 2.40−2.27 (m, 4H), 1.90−1.59 (m, 8H), 1.58−1.46 (m, 2H), 1.42 (s, 9H), 1.10 (d, J = 6.3 Hz, 6H).

***N*-((1s,4s)-4-Aminocyclohexyl)-2-(4′-(((3*S*,5*R*)-3,5-dimethyl-piperazin-1-yl)methyl)-2′-(morpholinomethyl)biphenyl-3-yloxy)-5-fluoronicotinamide 31.** To a stirred solution of **30** (0.300 g, 1 equiv) in CH_2Cl_2 (1 mL) was added 4 M HCl in 1,4-dioxane (1 mL, 10 equiv). The reaction mixture was stirred at rt for 1 h then concentrated to give **31** as the trihydrochloride salt (0.300 g, 99%).

dx.doi.org/10.1021/jm5001216 | J. Med. Chem. XXXX, XXX, XXX−XXX

^{1}H NMR (400 MHz, DMSO-d_6, δ): 8.28 (d, J = 7.5 Hz, 1H), 8.24 (d, J = 3.1 Hz, 1H), 8.02 (dd, J = 8.1, 3.1 Hz, 1H), 7.47 (t, J = 7.9 Hz, 1H), 7.39 (s, 1H), 7.35−7.38 (m, 1H), 7.22−7.28 (m, 3H), 7.19 (ddd, J = 8.2, 2.4, 0.9 Hz, 1H), 3.94−3.86 (m, 1H), 3.47−3.42 (m, 6H), 3.35 (s, 2H), 2.80−2.68 (m, 3H), 2.68−2.61 (m, 2H), 2.29−2.21 (m, 4H), 1.78−1.64 (m, 2H), 1.62−1.44 (m, 6H), 1.43−1.31 (m, 2H), 0.88 (d, J = 6.3 Hz, 6H).

2-(4′-(((3*S*,5*R*)-3,5-Dimethylpiperazin-1-yl)methyl)-2′-(morpholinomethyl)biphenyl-3-yloxy)-5-fluoro-*N*-((1s,4s)-4-(2-hydroxy-5-methylbenzamido)cyclohexyl)nicotinamide 12b [General Method H]. HOBt (0.473 g, 2 equiv), EDCI (0.592 g, 2 equiv), and Et_3N (0.215 mL, 1 equiv) were added to a solution of 2-hydroxy-5-methylbenzoic acid (0.470 g, 2 equiv) in THF (5 mL). The mixture was stirred for 10 min at rt then added to a solution of **31** hydrochloride (1.200 g, 1 equiv) and Et_3N (0.861 mL, 4 equiv) in THF (5 mL) and NMP (5 mL). The reaction mixture was stirred at rt overnight then evaporated to dryness and the residue dissolved in CH_2Cl_2 (150 mL) and washed with saturated aqueous $NaHCO_3$ and water, dried ($MgSO_4$), and concentrated. The crude product was purified by preparative HPLC and then by flash silica chromatography eluting with 4% 7 M NH_3 in MeOH in CH_2Cl_2 to give **12b** as a white solid (0.505 g, 43%). ^{1}H NMR (400 MHz, CD_3OD, δ): 8.10 (d, J = 3.1 Hz, 1H), 8.05 (dd, J = 8.0, 3.1 Hz, 1H), 7.56 (d, J = 1.8 Hz, 1H), 7.43 (t, J = 7.9, 7.9 Hz, 1H), 7.38 (s, 1H), 7.28−7.24 (m, 1H), 7.23−7.13 (m, 4H), 7.10 (dd, J = 8.4, 2.2 Hz, 1H), 6.72 (d, J = 8.3 Hz, 1H), 4.14−4.06 (m, 1H), 4.04−3.94 (m, 1H), 3.52 (s, 2H), 3.50−3.44 (m, 4H), 3.38 (s, 2H), 2.98−2.85 (m, 2H), 2.84−2.73 (m, 2H), 2.31−2.15 (m, 7H), 1.90−1.62 (m, 10H), 1.03 (d, J = 6.4 Hz, 6H). LRMS: m/z 765 $[M + H]^+$

***N*-((1s,4s)-4-(2-(4′-(((3*S*,5*R*)-3,5-Dimethylpiperazin-1-yl)-methyl)-2′-(morpholinomethyl)biphenyl-3-yloxy)-5-fluoronicotinamido)cyclohexyl)-4-methylthiazole-2-carboxamide 12a.** Prepared from 4-methylthiazole-2-carboxylic acid and **31** hydrochloride using general method H, as the trifluoroacetic acid salt in 70% yield. ^{1}H NMR (400 MHz, CD_3OD, δ): 8.14 (d, J = 3.1 Hz, 1H), 8.04 (dd, J = 7.9, 3.1 Hz, 1H), 7.74 (d, J = 1.4 Hz, 1H), 7.58 (t, J = 7.9 Hz, 1H), 7.51 (dd, J = 7.9, 1.5 Hz, 1H), 7.41−7.36 (m, 2H), 7.32 (dd, J = 8.0, 2.1 Hz, 1H), 7.20 (d, J = 7.7 Hz, 1H), 7.18−7.15 (m, 1H), 4.43 (s, 2H), 4.15−4.08 (m, 1H), 4.02−3.93 (m, 1H), 3.87−3.64 (m, 6H), 3.49−3.38 (m, 2H), 3.26−2.72 (m, 6H), 2.44 (s, 3H), 2.32−2.21 (m, 2H), 1.94−1.73 (m, 8H), 1.29 (d, J = 6.6 Hz, 6H). LRMS: m/z 756 $[M + H]^+$.

■ ASSOCIATED CONTENT

Ⓢ Supporting Information

Further synthetic details and full descriptions of biological methods used. This material is available free of charge via the Internet at http://pubs.acs.org.

■ AUTHOR INFORMATION

Corresponding Authors

*For C.D.S.: phone +1 781-228-0743; e-mail, chris.desavi2@astrazeneca.com.

*For R.J.C.: phone +46 31 77 61794; e-mail, rhona.cox@astrazeneca.com.

Author Contributions

C.D.S., R.J.C., A.R.C., M.R.D., A.M., L.C.M., and B.P. performed medicinal and synthetic chemistry. D.J.W. carried out modeling and property predictions. G.A., S.S.Y., P.S.G., and M.S.D. carried out biological profiling. R.R. carried out pharmacokinetic profiling. All authors contributed to the writing of this manuscript and have given approval to the final version.

Notes

All animal studies were carried out under licenses issued under the Animals (Scientific Procedures) Act 1986 following local ethical committee review.

The authors declare no competing financial interest.

■ ACKNOWLEDGMENTS

We acknowledge Pat Barton, Fiona Bell, Amanda Benjamin, Roger Bonnert, Juan Carrillo, John Collington, Rebecca Denton, Theresa Humphries, Fraser Hunt, Ray Hutchinson, Tony Ingall, Robert Jewell, Andy Kirk, Sarah Lever, Dermot McGinnity, Premji Meghani, Sandy Nicol, Victor Oreffo, Austen Pimm, Aaron Rigby, Andrew Robbins, Joanne Ross, Hitesh Sanganee, and Jerzy Schmidt.

■ ABBREVIATIONS USED

dppf, 1,1′-bis(diphenylphosphino)ferrocene; BAL, bronchoalveolar lavage; SPhos, 2-dicyclohexylphosphino-2′,6′-dimethoxybiphenyl; DIPEA, *N*,*N*-diisopropylethylamine; EDCI, *N*-(3-(dimethylamino)propyl)-*N*′-ethylcarbodiimide hydrochloride; HATU, *N*-[(dimethylamino)-1*H*-1,2,3-triazolo-[4,5-*b*]pyridin-1-ylmethylene]-*N*-methylmethanaminium hexafluorophosphate *N*-oxide; DRC, dose−response curve; ED_{80}, effective dose giving 80% inhibition; HOBt, 1-hydroxybenzotriazole hydrate; *i.t.*, intratracheal instillation; LENC, lowest effective nebulizer concentration; ND, not determined; NT, not tested; PBMC, peripheral blood mononuclear cell; PDE4, phosphodiesterase 4; T3P, propylphosphonic anhydride; RP HPLC, reverse phase HPLC; RMSE, root-mean-square error; SCX, strong cation exchange chromatography

■ REFERENCES

(1) From the *Global Strategy for the Diagnosis, Management, and Prevention of COPD*; Global Initiative for Chronic Obstructive Lung Disease (GOLD), 2014; available from: http://www.goldcopd.org/.

(2) Buist, A. S.; McBurnie, M. A.; Vollmer, W. M.; Gillespie, S.; Burney, P.; Mannino, D. M.; Menezes, A. M. B.; Sullivan, S. D.; Lee, T. A.; Weiss, K. B.; Jensen, R. L.; Marks, G. B.; Gulsvik, A.; Nizankowska-Mogilnicka, E. International variation in the prevalence of COPD (The BOLD study): a population-based prevalence study. *Lancet* **2007**, *370*, 741−750.

(3) *The Top 10 Causes of Death*; Fact Sheet no. 310; World Health Organization: Geneva, July 2013.

(4) Mathers, C. D.; Loncar, D. Projections of global mortality and burden of disease from 2002 to 2030. *PLoS Med.* **2006**, *3*, e442.

(5) Breunig, I. M.; Shaya, F. T.; Scharf, S. M. Delivering cost-effective care for COPD in the USA: recent progress and current challenges. *Expert Rev. Pharmacoecon. Outcomes Res.* **2012**, *12*, 725−731.

(6) Barnes, P. J.; Adcock, I. M. Glucocorticoid resistance in inflammatory diseases. *Lancet* **2009**, *373*, 1905−1917.

(7) Michalski, J. M.; Golden, G.; Ikari, J.; Rennard, S. I. PDE4: a novel target in the treatment of chronic obstructive pulmonary disease. *Clin. Pharmacol. Ther.* **2012**, *91*, 134−142.

(8) (a) Page, C. P.; Spina, D. Phosphodiesterase inhibitors in the treatment of inflammatory diseases. *Handb. Exp. Pharmacol.* **2011**, *204*, 391−414. (b) Beghè, B.; Rabe, K. F.; Fabbri, L. M. Phosphodiesterase-4 inhibitor therapy for lung diseases. *Am. J. Respir. Crit. Care Med.* **2013**, *188*, 271−278.

(9) (a) Boswell-Smith, V.; Page, C. P. Roflumilast: a phosphodiesterase-4 inhibitor for the treatment of respiratory disease. *Expert Opin. Invest. Drugs* **2006**, *15*, 1105−1113. (b) Heaslip, R. J.; Evans, D. Y. Emetic, central nervous system and pulmonary activities of rolipram in the dog. *Eur. J. Pharmacol.* **1995**, *286*, 281−290.

(10) (a) Giembycz, M. A. An update and appraisal of the cilomilast phase III clinical development programme for chronic obstructive pulmonary disease. *Br. J. Clin. Pharmacol.* **2006**, *62*, 138−152. (b) Rennard, S.; Knobil, K.; Rabe, K. F.; Morris, A.; Schachter, N.; Locantore, N.; Canonica, W. G.; Zhu, Y.; Barnhart, F. The efficacy and safety of cilomilast in COPD. *Drugs* **2008**, *68* (Suppl 2), 3−57.

(11) (a) Calverley, P. M. A.; Rabe, K. F.; Goehring, U.-M.; Kristiansen, S.; Fabbri, L. M.; Martinez, F. J. Roflumilast in symptomatic chronic obstructive pulmonary disease: two randomised clinical trials. *Lancet*

2009, *374*, 685−694. (b) Fabbri, L. M.; Calverley, P. M. A.; Izquierdo-Alonso, J. L.; Bundschuh, D. S.; Brose, M.; Martinez, F. J.; Rabe, K. F. Roflumilast in moderate-to-severe chronic obstructive pulmonary disease treated with long acting bronchodilators: two randomised clinical trials. *Lancet* **2009**, *374*, 695−703.

(12) Armani, E.; Amari, G.; Rizzi, A.; De Fanti, R.; Ghidini, E.; Capaldi, C.; Carzaniga, L.; Caruso, P.; Guala, M.; Peretto, I.; La Porta, E.; Bolzoni, P. T.; Facchinetti, F.; Carnini, C.; Moretto, N.; Patacchini, R.; Bassani, F.; Cenacchi, V.; Volta, R.; Amadei, F.; Capacchi, S.; Delcanale, M.; Puccini, P.; Catinella, S.; Civelli, M.; Villetti, G. A novel class of benzoic acid ester derivatives as potent PDE4 inhibitors for inhaled administration in the treatment of respiratory diseases. *J. Med. Chem.* **2014**, *57*, 793−816.

(13) Ting, P. C.; Lee, J. F.; Kuang, R.; Cao, J.; Gu, D.; Huang, Y.; Liu, Z.; Aslanian, R. G.; Feng, K.-I.; Prelusky, D.; Lamca, J.; House, A.; Phillips, J. E.; Wang, P.; Wu, P.; Lundell, D.; Chapman, R. W.; Celly, C. S. Discovery of oral and inhaled PDE4 inhibitors. *Bioorg. Med. Chem. Lett.* **2013**, *23*, 5528−5532.

(14) Vestbo, J.; Tan, L.; Atkinson, G.; Ward, J. A controlled trial of 6-weeks' treatment with a novel inhaled phosphodiesterase type-4 inhibitor in COPD. *Eur. Respir. J.* **2009**, *33*, 1039−1044.

(15) Tralau-Stewart, C. J.; Williamson, R. A.; Nials, A. T.; Gascoigne, M.; Dawson, J.; Hart, G. J.; Angell, A. D. R.; Solanke, Y. E.; Lucas, F. S.; Wiseman, J.; Ward, P.; Ranshaw, L. E.; Knowles, R. G. GSK256066, an exceptionally high-affinity and selective inhibitor of phosphodiesterase 4 suitable for administration by inhalation: in vitro, kinetic, and in vivo characterization. *J. Pharmacol. Exp. Ther.* **2011**, *337*, 145−154.

(16) Nials, A. T.; Tralau-Stewart, C. J.; Gascoigne, M.; Ball, D. I.; Ranshaw, L. E.; Knowles, R. G. In vivo characterization of GSK256066, a high-affinity inhaled phosphodiesterase 4 inhibitor. *J. Pharmacol. Exp. Ther.* **2011**, *337*, 137−144.

(17) Singh, D.; Petavy, F.; Macdonald, A. J.; Lazaar, A. L.; O'Connor, B. J. The inhaled phosphodiesterase 4 inhibitor GSK256066 reduces allergen challenge responses in asthma. *Respir. Res.* **2010**, *11*, 26.

(18) Woodrow, M. D.; Ballantine, S. P.; Barker, M. D.; Clarke, B. J.; Dawson, J.; Dean, T. W.; Delves, C. J.; Evans, B.; Gough, S. L.; Guntrip, S. B.; Holman, S.; Holmes, D. S.; Kranz, M.; Lindvaal, M. K.; Lucas, F. S.; Neu, M.; Ranshaw, L. E.; Solanke, Y. E.; Somers, D. O.; Ward, P.; Wiseman, J. O. Quinolines as a novel structural class of potent and selective PDE4 inhibitors. Optimisation for inhaled administration. *Bioorg. Med. Chem. Lett.* **2009**, *19*, 5261−5265.

(19) Jones, R. M.; Neef, N. Interpretation and prediction of inhaled drug particle accumulation in the lung and its associated toxicity. *Xenobiotica* **2012**, *42*, 86−93.

(20) Cooper, A. E.; Ferguson, D.; Grime, K. Optimisation of DMPK by the inhaled route: challenges and approaches. *Curr. Drug Metab.* **2012**, *13*, 457−473.

(21) Donnell, A. F.; Dollings, P. J.; Butera, J. A.; Dietrich, A. J.; Lipinski, K. K.; Ghavami, A.; Hirst, W. D. Identification of pyridazino[4,5-*b*]indolizines as selective PDE4B inhibitors. *Bioorg. Med. Chem. Lett.* **2010**, *20*, 2163−2167.

(22) (a) Lisius, A.; Nikitidis, G.; Sjö, P. Pyridopyrimidine derivatives as PDE4 inhibitors for the treatment of inflammatory and immune diseases. WO 2007/004958, January 11, 2007; *Chem. Abstr.* **2007**, *146*, 142674. (b) Austin, R.; Bonnert, R.; Hunt, F.; Nikitidis, G.; Sanganee, H.; Sjö, P.; Warner, D. Pyridopyrimidine derivatives and their use as PDE4 inhibitors. WO2007/108750, September 27, 2007; *Chem. Abstr.* **2007**, *147*, 406836.

(23) (a) Bonnert, R. V.; Burkamp, F.; Cox, R. J.; De Sousa, S.; Dickinson, M.; Hunt, S. F.; Meghani, P.; Pimm, A.; Sanganee, H. J. Chemical compounds 637. WO2008/084223, July 17, 2008; *Chem. Abstr.* **2008**, *149*, 176358. (b) Hartopp, P.; Johnson, T.; Sanganee, H. J. Combination comprising 6-fluoro-*N*-((1*S*,4*S*)-4-(6-fluoro-2,4-dioxo-1-(4-(piperazin-1-yl-methyl)biphenyl-3-yl)-1,2-dihydropyrido[2,3-*d*]-pyrimidin-3(4*H*)-yl)cyclohexyl)imidazo[1,2-*a*]pyridine-2-carboxamide or a salt. WO2010/004319, January 14, 2010; *Chem. Abstr.* **2010**, *152*, 144706.

(24) Andrews, G.; Cox, R. J.; De Savi, C.; Meghani, P.; Sanganee, H. J.; Warner, D. J. Phenoxypyridinylamide derivatives and their use in the treatment of PDE4 mediated disease states. WO2009/144494, December 3, 2009; *Chem. Abstr.* **2009**, *152*, 12149.

(25) *JMP* version 8.0; SAS Institute Inc.: Cary, NC, http//www.jmp.com.

(26) Bailey, S.; Gautier, E. C. L.; Henderson, A. J.; Magee, T. V.; Marfat, A.; Mathias, J. P.; McLeod, D. G.; Monaghan, S. M.; Stammen, B. L. C. Nicotinamide derivatives useful as PDE4 inhibitors. WO2003/068235, 21 August 2003; *Chem. Abstr.* **2003**, *139*, 197374.

(27) Cooper, A.; Potter, T.; Luker, T. Prediction of efficacious inhalation lung doses via the use of in silico lung retention quantitative structure−activity relationship models and in vitro potency screens. *Drug Metab. Dispos.* **2010**, *38*, 2218−2225.

(28) Free, S. M., Jr.; Wilson, J. W. A mathematical contribution to structure−activity studies. *J. Med. Chem.* **1964**, *7*, 395−399.

(29) Wood, D. J.; Buttar, D.; Cumming, J. G.; Davis, A. M.; Norinder, U.; Rodgers, S. L. Automated QSAR with a hierarchy of global and local models. *Mol. Inf.* **2011**, *30*, 960−972.

(30) Alcaraz, L.; Bailey, A.; Cadogan, E.; Connolly, S.; Jewell, R.; Jordan, S.; Kindon, N.; Lister, A.; Lawson, M.; Mullen, A.; Dainty, I.; Nicholls, D.; Paine, S.; Pairaudeau, G.; Stocks, M. J.; Thorne, P.; Young, A. From libraries to candidate: the discovery of new ultra long-acting dibasic β_2-adrenoceptor agonists. *Bioorg. Med. Chem. Lett.* **2012**, *22*, 689−695.

(31) Performed under contract at: Porsolt & Partners Pharmacology, Z.A. des Suhards, 53940 Le Genest-Saint-Isle, France.